

**OXYGEN SENSITIVITY OF
RUTHENIUM-DOPED SOL-GEL
DERIVED SILICA FILMS**

**Submitted for the Degree of
MASTER OF SCIENCE**

**Presented to
DUBLIN CITY UNIVERSITY**

by

**PAUL KIERNAN, B.Sc.
School of Physical Sciences
Dublin City University**

**Research Supervisor
DR. COLETTE MCDONAGH**

DECEMBER 1994

Abstract

The feasibility of an oxygen sensor based on the quenching of fluorescence of ruthenium complexes in the presence of oxygen was investigated. Porous sol-gel derived silica thin films deposited on a glass substrate by a dip-coating technique were impregnated with the fluorescent complexes Ruthenium(2,2-bipyridene)₃⁺⁺ and Ruthenium(4,7-diphenylphenanthroline)₃⁺⁺. Sol-gel film thickness, chemical composition and concentration of the fluorescent species within the film were optimised. The samples were excited by a CW Argon ion laser ($\lambda_{\text{ex}} = 488\text{nm}$) for fluorescent intensity measurements, and by a pulsed Nd-Yag laser ($\lambda_{\text{ex}} = 532\text{nm}$) for lifetime measurements. For each complex, both the fluorescent intensity and lifetime were quenched by oxygen.

The optical decay times were analysed using two methods: (a) Numerical Integration, and (b) Line stripping. Method (b) was favoured, and involved analysis in terms of one quenched and one unquenched fluorophore component, the latter arising from the fraction of ruthenium complex molecules which were inaccessible to oxygen. By taking intensity and lifetime measurements for known oxygen concentrations from 0 to 100%, intensity and decay time Stern-Volmer plots were produced for both complexes. The performance of both ruthenium complexes was compared and contrasted, and their suitability for use in optical oxygen sensors based on sol-gel entrapped fluorescent molecules was discussed.

Acknowledgements

I would like to take this opportunity to express by sincere gratitude to Dr. Colette McDonagh. Without her expertise, advice, knowledge and guidance this project would never have been completed. Thanks also to Dr. Brian MacCraith and to Aisling McEvoy, Ger O'Keeffe and Des Lavelle for their help and friendship.

I am grateful to Professor Eugene Kennedy at the School of Physical Sciences in Dublin City University for enabling me to attend various conferences and broaden my horizons and to Jackie and Marian, the secretarial staff, for their help during my time at D.C.U. Thanks must also go to Dr. John Twomey and his son Traolach, for their invaluable assistance. Finally, I must thank my parents for their help and support all along the way.

Declaration

I hereby certify that this material, which I now submit for assessment on the programme of study leading to the award of Master of Science is entirely my own work and has not been taken from the work of others save and to the extent that such work has been cited and acknowledged within the text of my work.

Signed Paul Kiernan
(Candidate)

Date 15th September 1994

Date

CONTENTS

	<u>Page</u>	
Abstract	(i)	
Acknowledgements	(ii)	
Declaration	(iii)	
Chapter 1	Introduction to Sol-Gel Glasses and Sensors	
1.0	Introduction	1
1.1	Sol-gel glasses	1
1.2	A brief history of oxygen sensors	2
1.3	Fluorosensors	3
1.4	Optical Fibre Sensors	4
1.5	Summary	6
	References	6
Chapter 2	Fluorescence	7
2.0	Introduction	7
2.1	Fluorescence	7
2.2	Quenching of fluorescence	9
2.3	Fluorescent lifetime and intensity	12
2.4	Ruthenium compounds	14
2.4.1	Ru (6ppy) ₃ ²⁺	15
2.4.2	Ru (Ph ₂ phen) ₃ ²⁺	18
2.5	Summary	19
	References	19
Chapter 3	The Sol-Gel Process	20
3.0	Introduction	20
3.1	Conventional and Sol-gel glasses	20
3.2	The Sol-gel process	21
3.2.1	Xerogel Production	24
3.3	Production of sol-gel thin films	29
3.3.1	The sol-gel dip process	30
3.4	Summary	32
	References	32

		<u>Page</u>
Chapter 4	Experimental	34
4.0	Introduction	34
4.1	Sol preparation	34
4.1.1	Substrate Coating	35
4.1.2	Thin film fabrication	35
4.1.3	Water-to-TEOS ratio (r)	37
4.1.4	Solution pH	37
4.1.5	Sol treatment prior to dipping	37
4.1.6	Film deposition	38
4.1.7	Film drying	39
4.2	Fluorescent species and concentration	39
4.2.1	Choice of fluorescent species	39
4.2.2	Fluorescent species and concentration	39
4.3	Sample setup	40
4.4	Fluorescent intensity measurements	40
4.4.1	Data acquisition	43
4.5	Lifetime measurements	43
4.5.1	Data acquisition	45
4.6	Fluorescent lifetime calculation	45
4.6.1	Line stripping	47
4.6.2	Numerical integration	48
4.7	Summary	52
	References	52
Chapter 5	Results	53
5.0	Introduction	53
5.1	$\text{Ru}(\text{bpy})_3^{2+}$	53
5.1.1	Optimum Dye Concentration	53
5.1.2	Fluorescent intensity vs oxygen concentration	55
5.1.3	Fluorescent lifetime vs oxygen concentration	57
5.2	$\text{Ru}(\text{Ph}_2\text{phen})_3^{2+}$	61
5.2.1	Optimum dye concentration	61
5.2.2	Fluorescent intensity vs oxygen concentration	63
5.2.3	Lifetime vs oxygen concentration	65
5.3	Choice of fluorescent species	66
5.4	Ageing temperature	70
5.5	Lifetime results	71
5.6	Film performance	72
5.7	Summary	72
	References	73
Chapter 6	Concluding Remarks	74
6.0	Introduction	74
6.1	Fluorescent intensity and lifetime	74
6.2	Suitability of the sol-gel matrix	77
6.3	Suitability of $\text{Ru}(\text{Ph}_2\text{phen})_3^{2+}$	78
6.4	Future developments	79
	References	80

Chapter 1 Introduction to sol-gel glasses and sensors

1.0 Introduction

The work carried out in this project is based on the fluorescence of a number of ruthenium complexes trapped within a microporous silica glass network prepared by a series of chemical reactions, collectively known as the Sol-Gel process. This chapter will briefly discuss sol-gel derived materials and their use in this project; and also serve as an introduction to oxygen sensors based on fluorescence quenching.

1.1 Sol-Gel Glasses

In recent years, sol-gel processes for glass making have gained scientific and technological importance. The prime technological importance of the sol-gel process is that it opens up the possibility of preparing homogeneous, 'high-temperature' glasses and glass-like ceramics at low temperatures. These methods are difficult to prepare by traditional methods because of (a) the high melting temperatures involved, and (b) a strong tendency of molten glasses to crystallise when cooling.

The sol-gel process, however, involves the use of an organic precursor in solution, which after a series of low temperature chemical reactions gives rise to an inorganic network in the form of a gel. Subsequent heat treatment of this gel results in a glass-like end product. Sol-gel derived materials play an important role in many technologies [1]. In particular, sol-gel derived thin films are now used as protective and antireflection coatings and as porous supports for catalysts, enzymes and sensors [2]. Advantages of the sol-gel process include low temperature processing and the possibility of tailoring materials properties, such as refractive index, density, and

porosity for specific purposes more easily than for conventional materials processing [3]. The sol-gel process lends itself very readily to coating deposition and thin film production; and it is in these areas that most commercial interests lie [4]. Thin films have been developed for optical, mechanical and electrical applications. It is important to realise that the sol-gel process is a series of chemical reactions which can be halted at different stages. For example, if a microporous sol-gel coating is desired, then the process can be stopped at an early stage, when the substrate to be coated can be dipped into a liquid sol. If on the other hand, large monolithic pieces of densified glass are required, then the process must be continued further so that the gel undergoes both chemical and high temperature physical drying treatment. In this project, porous sol-gel derived silica thin film coatings are used as supports for oxygen sensitive compounds.

1.2 A brief history of Oxygen Sensors

Almost all life on earth depends on chemical reactions with oxygen to produce energy. It is used in vast quantities in metallurgy, smelting and refining, and has many biomedical and environmental applications. It is very reactive, forming oxides with almost all known elements. It is desirable, and in some cases vital, therefore that methods and instruments exist that can determine oxygen concentrations. The first methods of determining oxygen concentrations used titration methods, the most common being the Winkler titration [5]. This is a slow method in that the oxygen concentration must remain constant throughout the entire process. It also consumes oxygen.

In 1956, a device that could measure the partial pressure of oxygen in solution by measuring the current flow between two electrodes was developed by L.C. Clark.

This type of sensor is the most commonly available today. Although quite successful, disadvantages inherent in this system include very slow response times (up to 30 minutes), thus ruling out the possibility of real-time *in situ* measurements. This sensor also consumes oxygen. The fluorescence based sensors, to be briefly discussed below, have overcome these limitations.

1.3 Fluorosensors

Fluorescence quenching can be defined as any process which decreases the fluorescence of a given substance. It can be caused by several processes, including that which results from collisional encounters between the fluorescing substance and quencher species. One of the most common collisional quenchers is molecular oxygen, which is known to quench nearly all fluorescent species. In 1968 Bergman developed an oxygen sensor based on the fluorescence quenching of long lifetime fluorescent compounds by oxygen [6]. Fluorothane, a strongly fluorescent polycyclic aromatic hydrocarbon (PAH) was adsorbed on a porous glass support (in this case Vycor glass) and excited with a UV light source. The resulting fluorescence was strongly quenched by oxygen, and was measured with a photocell.

The fluorescence of a variety of other PAH's is known to be quenched by molecular oxygen. Among these, pyrene, and to a lesser extent pyrenebutyric acid (PBA) are probably most efficiently quenched by virtue of their long radiative lifetimes (>100 ns). PBA in a silicone polymer has been employed as a support for the fluorescent species. It was noticed that the dye was slowly 'washed' from its polymeric support, but this problem was overcome by immobilisation in a porous glass [7].

Aside from PAH's, which have been applied in covalently immobilised, surface-adsorbed, and polymer-dissolved form, **metal organic complexes** of ruthenium have

been used as oxygen indicators for several reasons: (a) they have relatively long lifetimes (up to 5 microseconds), (b) they have favourable excitation wavelengths (450 to 490 nm) which makes them excitable by the argon ion laser line and blue L.E.D.s and (c) they display relatively large Stokes' shifts (the difference in wavelength between the absorption and emission spectra) which minimises effects caused by incident radiation scattering.

Oxygen quenches both the intensity and lifetime of the fluorescence of these complexes. The lifetime is defined as the time taken for the initial fluorescence to drop to $1/e$ of its initial value. For long excited state lifetime fluorescent compounds, the probability of an encounter that will result in quenching (in this case, collision with an oxygen molecule) is much higher than for one with a short lifetime. Thus the long lifetimes of the metal-organic indicators of the type used in this project render them particularly useful for lifetime studies.

As will be discussed later, lifetime based sensors have certain advantages over intensity based devices. These include negligible signal drift due to loss of fluorophore, excellent long term stability, and immunity to excitation source and photodetector fluctuations.

1.4 Optical Fibre sensors

The major advantages of optical fibre based sensors over conventional oxygen sensors are (1) their inherent small size; (2) due to the fact that light is the information carrier that they are less susceptible to outside interference; and (3) unlike electrode based sensors, they do not consume oxygen. Some of the advantages of optical fibre based sensors are discussed briefly below.

(1) Size:

Optical fibres used in sensor applications will usually have diameters ranging from 100 to 300 microns, and this small size is of great advantage when dealing within restricted environments. Fibre length and flexibility also are of significant importance, allowing for remote sensing in places difficult to access. The possibility of distributed sensing at different parts of a long fibre also exists.

(2) Cost:

The price of commercial optical fibre has fallen dramatically over recent times, and therefore the costs of the short lengths of fibre used in sensing applications are negligible. The only significant costs are in the instrumentation associated with the light source and detection systems; though with the use of L.E.D.s and photodiodes, these costs are rapidly decreasing.

(3) Safety:

As light is the information carrier, no danger associated with conventional sensors (such as electric sparks) exist with fibre optic sensors. This is particularly important where high concentrations of oxygen are used, or when the sensing environment contains flammable gases.

Optical based oxygen sensors are usually highly specific, with no interferences found for water vapour, nitrogen, noble gases, carbon dioxide, and methane and higher alkanes. These sensors have been developed over the last twenty years as fast, sensitive, durable and safe sensors

1.5 Summary

This chapter briefly introduced the sol-gel derived glasses, and some of their advantages over those produced by conventional means. The history of oxygen sensors, including those operating on fluorescence based principles and the use of optical fibres in sensing applications was also discussed.

References

- [1] "Chemical processing of advanced materials"; L.L. Hench, J.K. West, Wiley, New York 1992.
- [2] "Sol-gel process in glass science and technology"; S.P. Mukherjee. *Journal of Non-Crystalline Solids*, 42, 1980, pp 477-86.
- [3]"Sol-Gel Science "; C.J.Brinker and G.W.Scherer, Academic Press, New York , 1989.
- [4] "Sol-gel technology for thin films, fibers, preforms, electronics and speciality shapes"; edited by L. Klein. Published 1988 by Noyes Publications.
- [5] "Determination of dissolved oxygen by the Winkler Method"; D.Skoog and J.West. *Fundamentals of Analytical Chemistry*, Vol. 4, pp 772-3, 1967.
- [6] "Determination of oxygen concentrations by luminescence quenching of a polymer immobilised transition metal complex"; J. Demas, K. Bacon. *Analytical Chemistry*, Vol. 59, 1987, page 2780.
- [7] "Fibre optic Chemical Sensors and Biosensors"; edited by O.S. Wolfbeis Vol. 11, page 31. Published by Wiley 1986.

Chapter 2

Fluorescence

2.0 Introduction

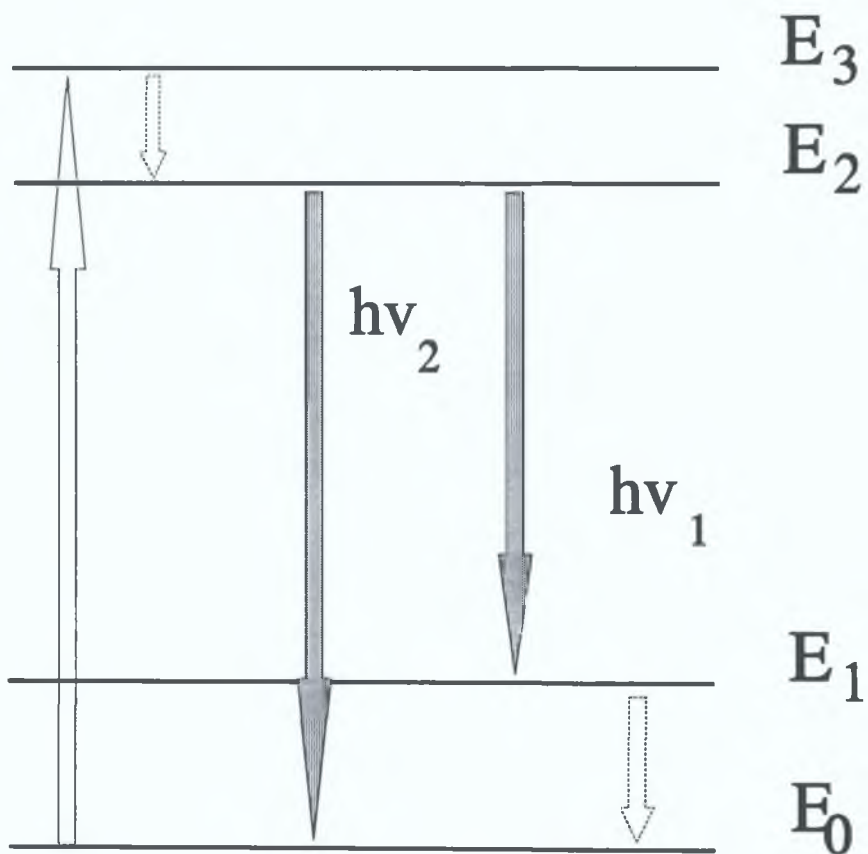
The basic principles of fluorescence and fluorescence quenching are explained in the following chapter. The reader will also be introduced to the fluorescent complexes investigated, and their properties of interest in sensing applications.

2.1 Fluorescence

Fluorescence is the non-thermal emission of electro-magnetic radiation from a molecule which has been placed in an excited state by, for example, absorption of photons, electron collisions, and chemical or biomolecular reactions.

When the fluorescent species is excited by the absorption of light, the emitted photons are of lower energy (or longer wavelength) than the absorbed photons. This is due to the energy losses encountered during inter-electronic level crossover events. Fundamental excitation and emission process are shown in figure 2.1, where E_0 represents the ground (or unexcited) state and E_1, E_2, E_3 represent energies of excited states. If a molecule, with ground state energy level E_0 is excited by an incoming photon, it can be raised to an excited state, E_3 . The absorbed energy can be released either radiatively or non-radiatively. Non-radiative decay (usually by the release of energy as heat through phonon emission) occurs if the energy level gaps are small, as between E_3 and E_2 .

For the fluorescent complexes used in this work, the radiation decay is either from a singlet state or a triplet state.[1],[2] If the electron in the higher energy orbital has a spin orientation opposite to the electron in the lower orbital, then the state is



Key:



-  : Radiative relaxation.
-  : Non-radiative relaxation.

Figure 2.1
Excitation and Decay in an
Optically Active material

singlet excited and the electrons are "paired". For the excited triplet state however, the electrons are unpaired, and their spin orientation the same. Fluorescence is usually the emission resulting from the return of the paired electron to the ground state. Such transitions are quantum mechanically allowed, with emission rates as high as 10^8 per second, resulting in fluorescent lifetimes of approximately 10 ns.[2] Emission also occurs when a triplet state excited electron returns to a singlet ground state. These transitions, between states of different multiplicity, are "forbidden" and so emission rates are slow, and fluorescence lifetimes are longer [2].

Radiative decay will occur if the gap between energy levels is above a critical value [1]. The molecule will decay radiatively from level E_2 to E_1 or E_0 . If the material decays radiatively to level E_1 , then it will decay further, non-radiatively, through the small gap to the ground state.

In figure 2.1, the emitted photons have energies described by

$$h\nu_1 = E_2 - E_1,$$

$$h\nu_2 = E_2 - E_0,$$

where ν is the frequency of the fluorescent radiation, and h is Planck's constant.

The two parameters of interest in this work are the fluorescent intensity and the fluorescent lifetime. Both properties have been used in sensor applications, and they will be discussed later in this chapter.

2.2 Quenching of fluorescence

Fluorescence quenching is described as any process which causes the non-radiative loss of energy from a molecule in the excited state [1].

There are two forms of fluorescence quenching, static quenching and dynamic

quenching. Static quenching is due to complex formation, where a complex is formed between the fluorophore and quencher, this complex being non-fluorescent. Dynamic quenching occurs when a free molecule, (in this case oxygen), interacts with the excited fluorophore resulting in the non-radiative transfer of energy. It is dependent on the concentration of the quenching molecule, and on the mobility or rate at which the quencher can diffuse to the excited molecule.

Both the intensity and lifetime of the fluorescent radiation decrease with increasing quencher concentration. The observed lifetime depends on the radiative and non-radiative decay rates as in the following equation: (Note :decay rate = $1/\tau$)

$$\frac{1}{\tau_{\text{obs.}}} = \frac{1}{\tau_{\text{rad.}}} + \frac{1}{\tau_{\text{non-rad.}}} \quad \dots\text{Eqn.1}$$

As the concentration of quencher increases, the non -radiative decay rate increases and thus the observed lifetime will decrease. The lifetime of the excited molecule is dependent on the static quenching constant and the dynamic quenching rate coupled with the quencher concentration. The Stern-Volmer equation describes how these factors interact mathematically, and is derived below [1].

If a bulk fluorophore is excited by an incident pulse of light, the excited molecules will relax with a rate constant K . K is the sum of several rate constants, such that:

$$K = K_e + K_i + K_q[A] \quad \dots\text{Eqn.2}$$

where K_e = the rate constant for emission of a photon;

K_i = the rate constant for internal conversion of the excitation energy;

K_q = the rate constant for transfer of energy to the quenching agent;

and $[A]$ = the concentration of quencher molecules in the bulk fluorophore.

If the excited molecule relaxes by fluorescence emission only, then the number of

excited fluorophore molecules, N , remaining at a time t after the excitation pulse is given by:

$$N = N_0 \cdot e^{-k_{et}t} \quad \dots \text{Eqn.3}$$

where N_0 is the number of excited fluorophores just after the excitation pulse.

The fluorescence quantum yield, Q , defined as the ratio of the number of photons emitted by the fluorophore to the number of excitation photons absorbed can be expressed as follows:

$$Q = \frac{K_e}{K_e + K_i + K_t \cdot [A]} \quad \dots \text{Eqn.4}$$

If fluorescence is the only means of relaxation, then by definition K_i and K_t are equal to zero and Q will equal 1. In the presence of a quencher however, where other relaxation processes exist, Q diminishes. A ratio of Q_0 (the quantum yield in the absence of oxygen) to Q (the quantum yield under a quencher concentration $[A]$) can be expressed as follows:

$$\frac{Q_0}{Q} = \frac{K_e / (K_e + K_i)}{K_e / (K_e + K_i + K_t \cdot [A])} = 1 + a \cdot K_t \cdot [A] \quad \dots \text{Eqn.5}$$

where: $a = \frac{1}{(K_e + K_i)}$

Equation 5 is the Stern-Volmer equation. It can be shown that

$$\frac{Q_0}{Q} = \frac{I_0}{I}$$

where I_0 is the fluorescent intensity in the absence of quencher, and I is the intensity in the presence of quencher, and so:

$$\frac{I_0}{I} = 1 + b \cdot [A] \quad \dots \text{Eqn.6}$$

Similarly,

$$\frac{I_0}{\tau} = 1 + b \cdot [A] \quad \dots \text{Eqn.7}$$

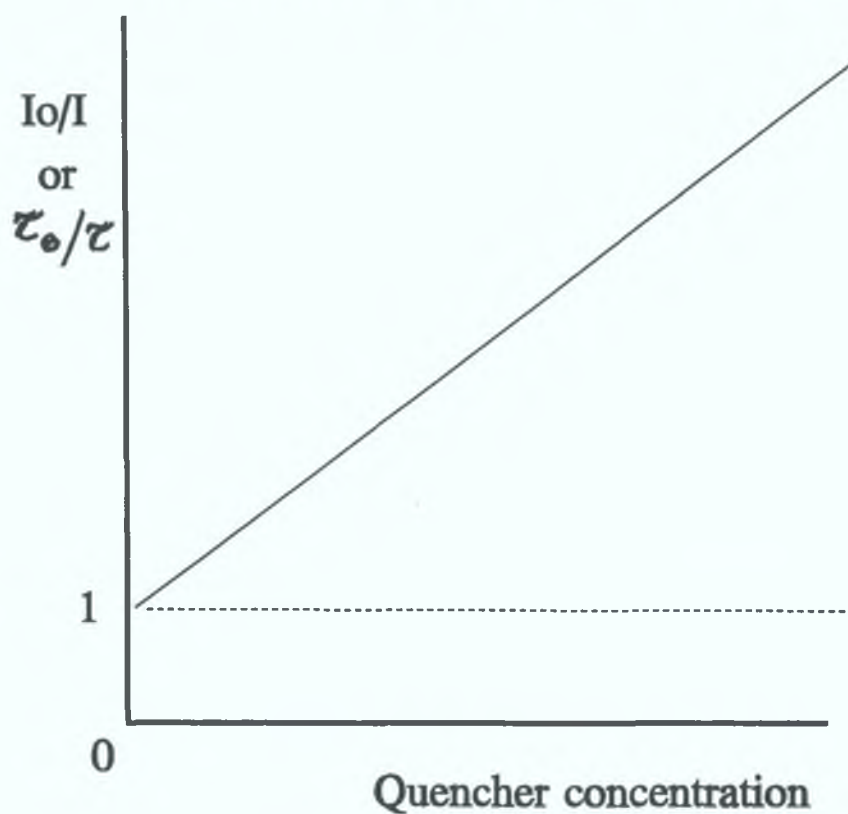
where τ_0 and τ are the fluorescent lifetimes in the absence and presence of quencher respectively and b is the Stern-Volmer quenching constant.

If the ratio of quencher-free intensity (or lifetime) to intensity (or lifetime) at a given quencher concentration, is plotted against quencher concentration then a linear plot is obtained. Such a plot is shown in Figure 2.2, where it can be seen that the line passes through the point (0,1) on the intensity axis.

2.3 Fluorescent Lifetime and Intensity

Both the fluorescent intensity and lifetime of the Ruthenium complexes used in this project are quenched in the presence of oxygen, and so oxygen sensors can be based on changes in either (or both) properties. While changes in intensity are more straightforward to measure, lifetime based sensors offer certain decisive advantages. Because the decay time is independent of fluorophore concentration, there is no signal drift due to either photobleaching of the fluorophore, or leaching of the fluorophore from its support matrix. Photobleaching and photodegradation of the fluorescent species can occur if the intensity of the excitation radiation is too high, or if the fluorophore is exposed to the radiation for long periods of time. Leaching of the fluorophore from its support can be a major problem if the sensor is used under aqueous, very humid or similarly harsh conditions. The fact that the lifetime is not affected implies greater long-term stability, and a more diverse range of applications, than intensity based sensors. Fluctuations in the excitation source, or in detector stability, which could give rise to false oxygen concentration readings, have no effect on a lifetime based system because it is not the absolute intensity that

Theoretical Stern/Volmer plot.



I_0 = Intensity in absence of quencher.

τ_0 = Lifetime in absence of quencher.

Figure 2.2

is measured, but the lifetime of the fluorescent radiation. In the case of optical fibre sensors, where tens of metres of fibre optic cable may be used for remote sensing, fibre degradation, resulting in a weakened signal, could give rise to false oxygen readings in an intensity based system. Again this will not affect lifetime measurements. Lifetime quenching is governed only by dynamic quenching processes, while fluorescent intensity can be affected by static quenching also.

Finally, there are several ways that the lifetime of the fluorescence can be measured, including pulse excitation and measurement of the resultant fluorescent decay, and phase shift techniques.

2.4 Ruthenium compounds

Increasingly, transition metal complexes find use in sensing applications, in particular complexes with the Platinum Metals (Ruthenium, Osmium, Rhenium, and Rhodium) [2]. These complexes are usually highly fluorescent, with high quantum yields and long lifetimes. They are usually easily excited, with absorption spectra peaking in the near Ultra-Violet or blue visible wavelength range. Due to large Stokes Shifts the resultant fluorescence is usually easy to observe. Thus relatively inexpensive equipment can be used for excitation and detection. Of the metals mentioned above, ruthenium is probably the most suitable for use in sensor applications. Complexes formed with ruthenium are more emissive than those formed with osmium, and for complexes of ruthenium with bipyridine, a strong fluorescent signal peaking at 610 nm is observed. Rhodium bipyridine, although highly emissive and with a lifetime of the order of tens of milliseconds at very low temperatures (77 K), has almost no emission at room temperature, and thus would be of little use for sensor applications. Some of the properties of ruthenium, and the ruthenium complexes used in this

project are discussed below.

Ruthenium was discovered in 1844 by G. Claus, and accepted as the newest Platinum Metal Group metal in 1845 by J.J. Berzelius [3]. Before ruthenium compounds found use in fluorescence applications, the metal was used principally as a hardener for palladium or platinum, and as a catalyst for hydrogenation reactions [4]. The luminescent properties of certain ruthenium compounds are exploited in sensor applications, where sensor operation is based on the quenching of fluorescence in the presence of oxygen [5].

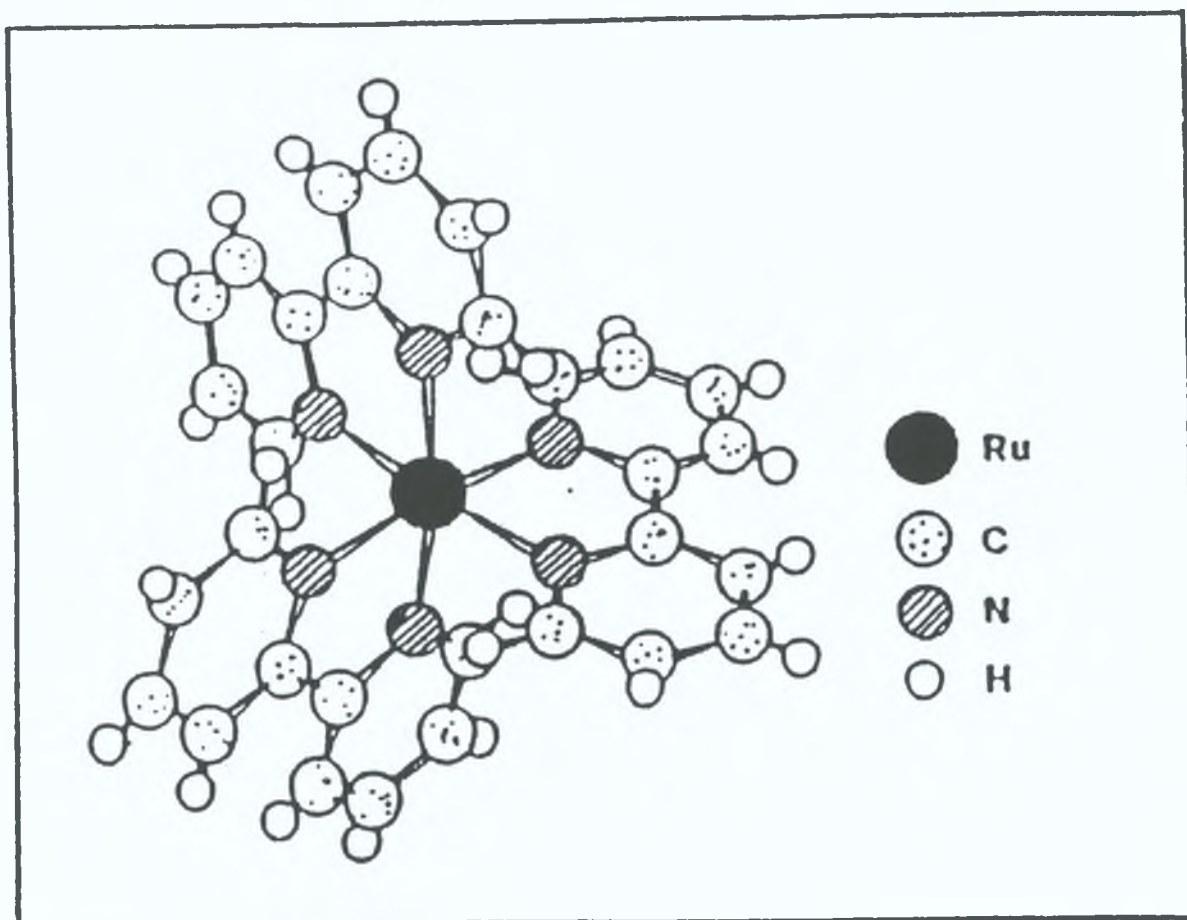
The two compounds used in this project were $\text{Ru}(2,2\text{-bipyridine})_3^{++}$ (or $\text{Ru}(\text{bpy})_3^{++}$) and $\text{Ru}(4,7\text{-diphenylphenanthroline})_3^{++}$ (or $\text{Ru}(\text{Ph}_2\text{phen})_3^{++}$). Both compounds are derived from RuCl_3 , a compound obtained by reacting the ruthenium metal with chlorine at 450°C . Both are highly emissive and their spectroscopic properties are discussed below.

2.4.1 $\text{Ru}(\text{bpy})_3^{++}$

The transition metal complex $\text{Ru}(\text{bpy})_3^{++}$ is classed as a bidentate heterocyclic complex, and its structure is shown in Figure 2.4.1. Its absorption spectrum has maxima at 454, 428, 345, 323, 285, 250 nm, and its fluorescence emission peaks at 610 nm. Figure 2.4.2 (a) shows the fluorescence spectrum.

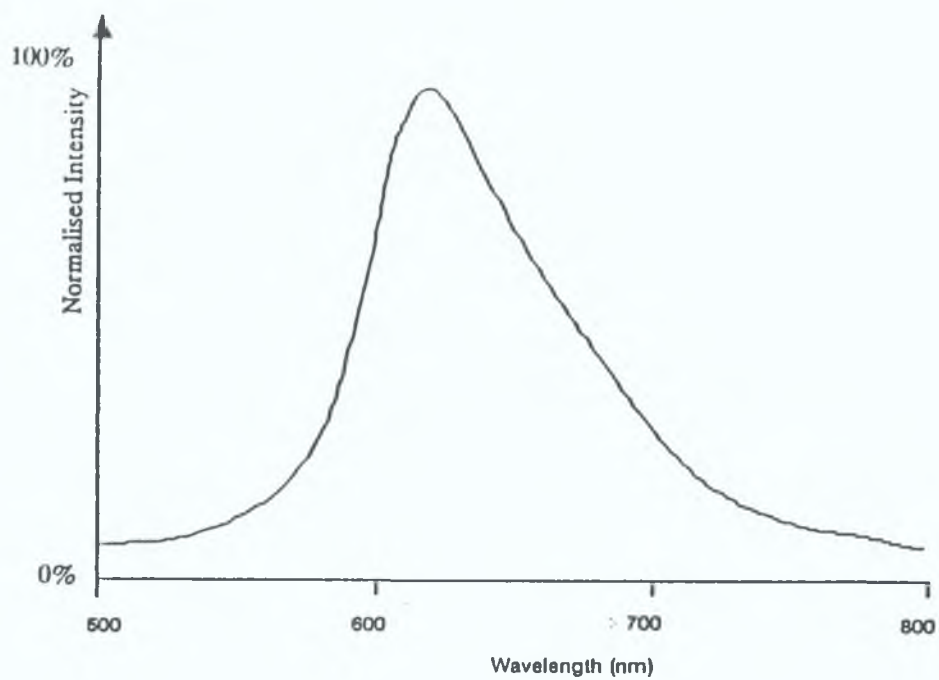
The nature of the fluorescence of $\text{Ru}(\text{bpy})_3^{++}$ is attributed to the metal to ligand charge transfer (MLCT) of an electron residing on a single bipyridyl ligand [6]. A small interaction between the ligands allows the migration of the excited electron from one ligand to another on a nanosecond timescale. The MLCT state is quite long lived, giving the fluorophore a relatively long lifetime. Non-radiative relaxation of the excited state occurs due to triplet-triplet quenching by oxygen. The process of

Figure 2.4.1

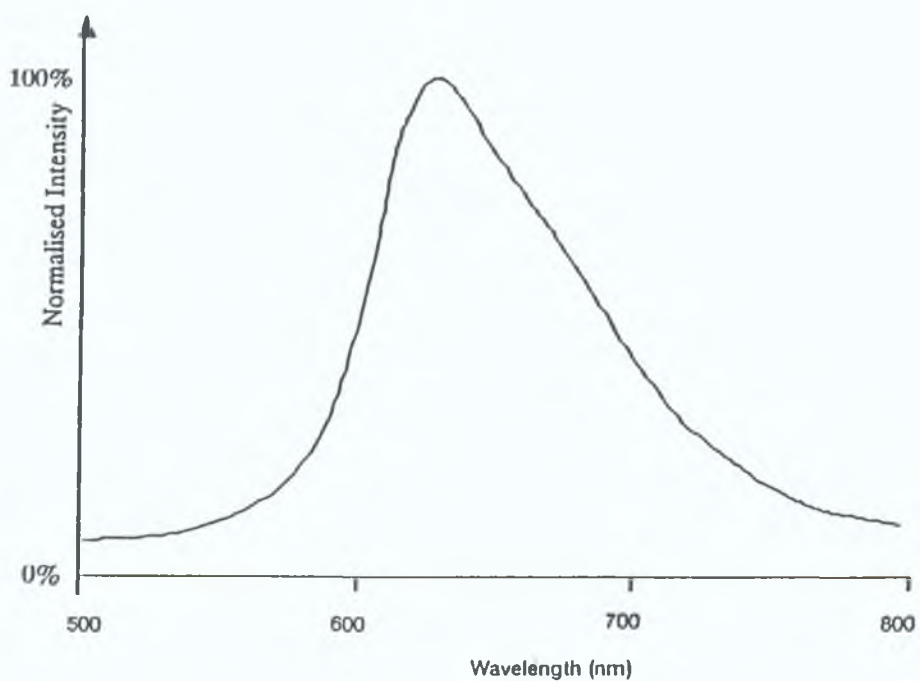


Structure of Ru(2,2-bipyridine)₃²⁺

Figure 2.4.2 Emission spectrum for $\text{Ru}(\text{bpy})_3^{++}$



Emission spectrum for $\text{Ru}(\text{Ph}_2\text{phen})_3^{++}$



dynamic fluorescence quenching is usually interpreted in terms of formation of a charge-transfer complex, or oxciplex, upon collision of oxygen and the excited fluorophore. As a result, non-radiative relaxation of the oxciplex gives the ground state species, which dissociates to give the fluorophore and oxygen. It is important to stress that no oxygen is consumed in this process.

The compound is a suitable candidate for use in oxygen sensing applications for several reasons. It has a relatively long lifetime and changes in the lifetime due to oxygen quenching are easily observed. Secondly, the excited state of $\text{Ru}(\text{bpy})_3^{++}$ is very selective in that it is quenched by only a small number of chemical species. Thirdly, it is easily incorporated into a porous sol-gel matrix.

2.4.2 $\text{Ru}(\text{Ph}_2\text{phen})_3^{++}$

This complex is quite similar in structure to $\text{Ru}(\text{bpy})_3^{++}$, resulting in similar spectroscopic and photochemical properties with absorption peaks at 460, 417, 263, and 224 nm, and a fluorescence emission peak at 610 nm. Figure 2.4.2 (b) shows the fluorescent emission spectrum of the complex.

It offers some advantages over the $\text{Ru}(\text{bpy})_3^{++}$ molecule however. Like $\text{Ru}(\text{bpy})_3^{++}$, it is highly emissive and has the MLCT state as the emitting state. However, it has more triplet character in the emitting state, and hence has a longer lifetime (approx 5.5 microseconds) and consequently, a larger quenching constant [7]. Also, the excited state of the $\text{Ru}(\text{Ph}_2\text{phen})_3^{++}$ is much less photoreactive than $\text{Ru}(\text{bpy})_3^{++}$, and thus is more stable sensing dye which is less susceptible to photobleaching.

2.5 Summary

The general principles of fluorescence and fluorescence quenching were discussed in this chapter. These included the two fluorescent properties of interest, namely fluorescent lifetime and intensity, and their respective merits. The Stern-Volmer equation, which allows one to relate quencher concentration to values of the above properties was derived for intensity and lifetime. The ruthenium complexes investigated in this work and their suitability for use in oxygen sensing applications were also described.

REFERENCES

- [1] "Principles of Fluorescence Spectroscopy"; edited by J. Lakowicz. Published by Plenum Press, 1983.
- [2] "Design and Applications of highly luminescent Transition Metal complexes"; J. Demas, B. DeGraff. Analytical Chemistry, Vol. 63, No. 17, 1991.
- [3] "Rare Metals Handbook"; C. Hampel, pp 304-333. Published by Skokie, Illinois, 1961
- [4] "Advances in Catalysis"; H. Gilman and D. Cohn, New York Academic Press Inc., Vol. 9, 1957, pp 733.
- [5] "Ruthenium doped sol-gel derived silica films - oxygen sensitivity of optical decay times"; P. Kiernan, C. McDonagh, B. Mac Craith, K. Mongey. Journal of Sol-Gel Science and Technology, 1994, Vol.2, page 513-518.
- [6] "Photochemistry of $\text{Ru}(2,2\text{-bipyridine})_3^{2+}$ "; Durham, Casper, Nagle and Meyer, Journal of American Chemistry Society, Vol 104, 1982, pp 4803-4810.
- [7] "A Fibre Optic Oxygen Sensor based on the Fluorescence Quenching of Ruthenium Compounds"; A.K. Geissel. MSc. Thesis, Dublin City University, Unpublished.

Chapter 3

The Sol-Gel Process

3.0 Introduction

The Sol-gel process is a low temperature, low cost method for the production of tailor-made glasses. The process by which these glasses is made are discussed in this chapter, as well as some of their properties and their advantages over conventional glasses.

3.1 Conventional and Sol-Gel glasses

The earliest known manufactured glass was made in Mesopotamia in the third millennium B.C. It was shaped by moulding or core-dripping, and this technique was used until the invention of glass blowing by Syrian craftsmen in the first century B.C. [1].

Conventional glasses are formed by the rapid cooling of certain molten liquids, so that they fail to crystallise, but instead retain an amorphous structure. This process is a high temperature one, involving the melting of starting mixtures in furnaces at temperatures up to 1500 °C. Shaping these glasses can be a complicated procedure. Depending on the composition of the molten glass, casting, rolling or drawing techniques are used. Sol-gel glasses offer many advantages over conventional glasses. Probably the most significant of these is that a sol-gel glass can be manufactured from a liquid precursor at room temperature. This also enables the production of thin films and coatings with relative ease.

Because the sol-gel process is a series of steps in a controllable chemical reaction, the properties of the end products can be tailored to suit specific needs and purposes [2]. Parameters such as density, surface area, porosity and pore size, optical transmission and refractive index can all be controlled through suitable processing. Hence, applications of the sol-gel process range from antireflective coatings to low expansion insulating glasses.

This project, in investigating the feasibility of an oxygen sensor based on ruthenium doped sol-gel coatings, exploits the porous nature of sol-gel derived glasses and the ease with which these coatings can be produced.

3.2 The Sol-Gel process

Although the Sol-Gel process can be used to produce monolithic glass and thin films from organic precursors containing elements such as Barium, Titanium and Zirconium, this project is concerned primarily with sol-gel derived SILICA glass coatings.

There are three main methods of sol-gel glass production:

1. Gelation of a solution of colloidal powders;
2. Hydrolysis and polycondensation of alkoxide precursors followed by hypercritical drying;
3. Hydrolysis and polycondensation of alkoxide precursors, followed by aging and drying under ambient conditions [3].

In the treatment which follows, sols are defined as dispersions of colloidal particles in a liquid, where colloids are solid particles with diameters of 1-100 nm. Gels are interconnected, rigid networks with pores of sub-micron dimensions and polymeric chains whose average length is greater than a micron.

Figure 3.1 shows the structural development of sol-gel derived silica, and the different steps involved. A silica gel may be formed by network growth from an array of discrete colloidal particles (as in method 1 above), or by the formation of an interconnected three dimensional network, by the simultaneous hydrolysis and polycondensation of an organometallic precursor (methods 2 and 3) [4].

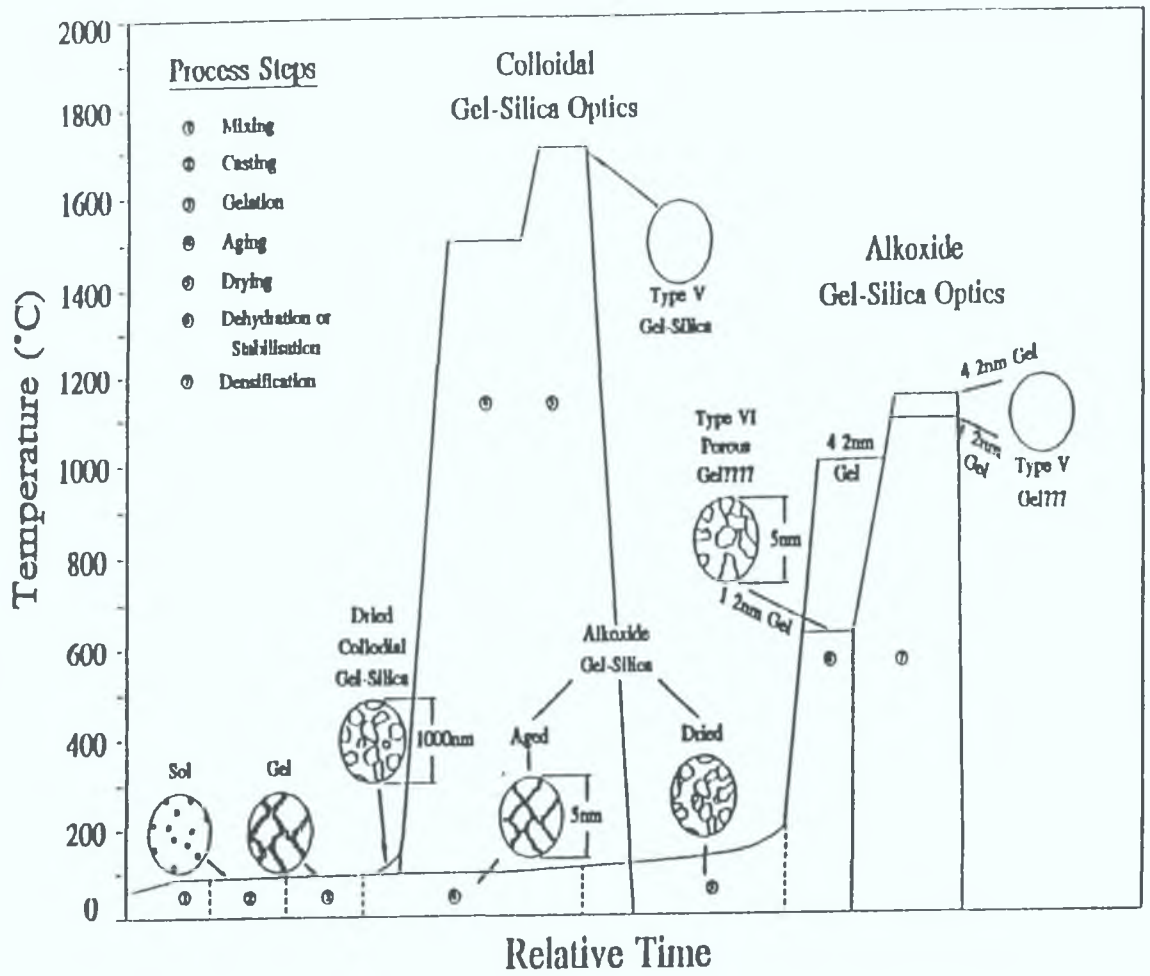
For the latter two methods, common precursors include $\text{Si}(\text{CH}_3)_4$, $\text{Si}(\text{C}_2\text{H}_5)_4$, and $\text{Si}(\text{C}_3\text{H}_7)_4$. $\text{Si}(\text{C}_2\text{H}_5)_4$ is tetraethylorthosilicate, or TEOS, the precursor used in this project. Hydrolysis occurs on mixing with water. The hydrolysed Si tetrahedra undergo a condensation reaction forming Si-O-Si bonds. Additional SiOH tetrahedra link and an SiO_2 network is formed [5]. Water and alcohol are expelled by the reaction mechanism, and will "inhabit" the porous network as a pore liquid.

Method 2 requires drying under hypercritical conditions. Here, the pore liquid is removed as a gas phase from the interconnected solid gel network. Under hypercritical conditions, the network does not collapse, and low density gels (as low as 80 kgm^{-3}) with pore volumes as high as 98%, termed Aerogels, are produced.

If the pore liquid is removed under ambient or near ambient conditions by thermal evaporation and shrinkage occurs, then the resultant gel is termed a xerogel.

This method, method 3, was used in the synthesis of all gels made during this project.

After gelation, further treatment can be carried out on monolithic gels to produce a final densified glass. Referring to Figure 3.1, step 4 represents the aging of a gel. The gel is immersed in a liquid for time periods varying from hours to days. Condensation continues, along with localised solution and reprecipitation of the gel network. This increases the size of the interparticle necks and thus the strength of the gel is increased. This strengthening is vital to resist cracking during the next step,



Structural development of Sol-Gel derived silica.

FIGURE 3.1

drying.

Drying occurs at temperatures between 100°C and 200°C, and it is at this stage that pore liquid is removed from the interconnected pore network. Large capillary stresses can occur (in pores of diameter < 20 nm) at this stage, and to prevent catastrophic cracking, certain techniques can be used to decrease the liquid surface energy. These include the addition of surfactant reagents, hypercritical drying (as in Method 2 above), and obtaining monodisperse pore sizes by controlling the rates of hydrolysis and condensation.

The next step, dehydration and chemical stabilisation involves the removal of physisorbed water from the pore network, and the elimination of surface silanol or Si-OH groups. These steps are necessary to produce a transparent end product after high temperature densification. At temperatures up to 400°C, the dehydration process is reversible, but above 400°C, shrinkage and densification occurs.

Densification is usually carried out at temperatures up to 1400°C. Pores are eliminated by collapsing of the network, and the resulting glass has a density equivalent to fused Quartz or silica.

3.2.1 Xerogel production

A schematic representation of the process is shown in Figure 3.2.

Basically, the precursor is mixed with water to form a homogeneous solution which undergoes a simultaneous hydrolysis and polycondensation reaction to form a homogenous non-crystalline gel. Low temperature thermal treatment of this gel (to remove excess water and alcohol) gives a porous xerogel. Further high temperature heating and sintering will result in a densified glass [6].

In this project, the precursor used was tetraethylorthosilicate, or TEOS, with

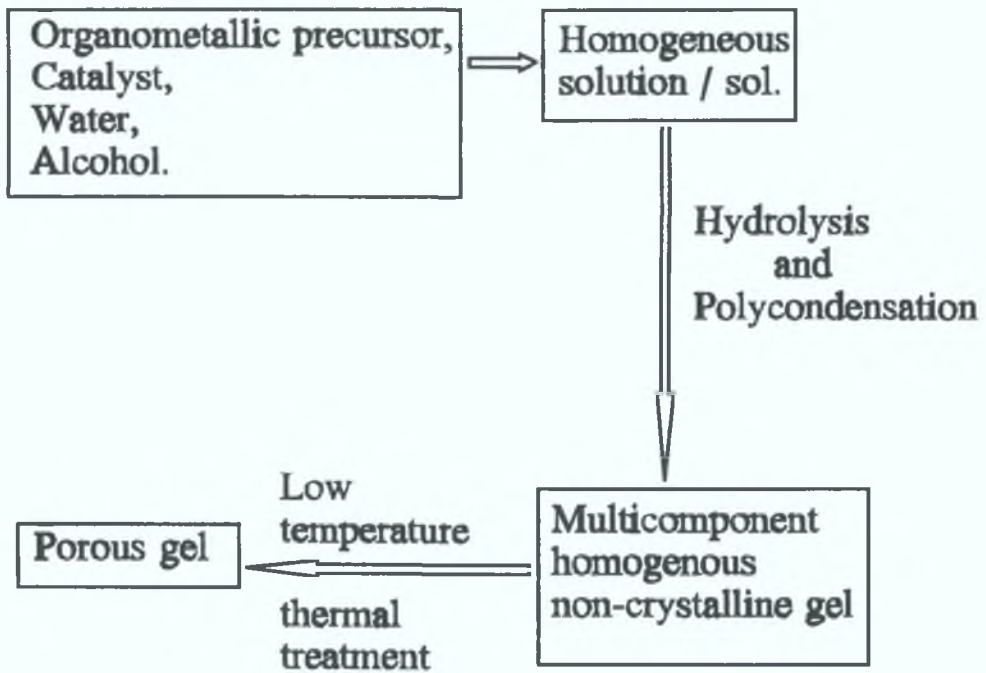


Figure 3.2
A schematic representation of the
Sol-Gel process.

hydrochloric acid as the catalyst. The TEOS is hydrolysed by mixing with water, (ethanol is added because TEOS and water are only partly miscible), and the reaction proceeds initially as follows:



The hydrolysed silica tetrahedra interact in a condensation reaction, forming silica chains with the elimination of water. Linkage of additional SiOH tetrahedra occurs as a condensation reaction (see Figure 3.3) and eventually results in an SiO₂ network. The hydrolysis and condensation reactions are initiated at numerous sites within the TEOS/water solution as mixing occurs. When sufficient Si-O-Si bonds are formed, they respond cooperatively as colloidal particles, or a sol.

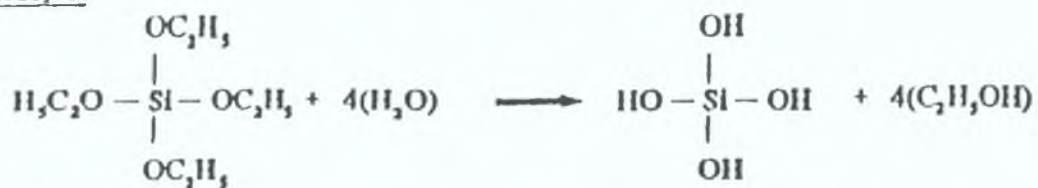
Sol particle size, and the extent of cross linkage within the particles depend on the pH of the starting solution, and on the molar ratio, *r*, of water to TEOS. With the progression of time, the colloidal particles and condensed silica link to become a three dimensional network or gel. Thus, the physical characteristics of this gel also depend greatly on particle size and extent of cross linkage prior to gelation.

Many factors affect the physical characteristics of the final gel; these include solution pH, type of catalyst, gelling temperature and drying methods.

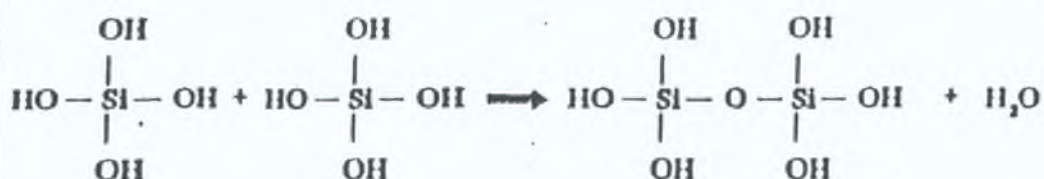
Solution pH affects the sol-gel polymerisation in two ways: (1) it modifies the rates of hydrolysis and condensation reactions, and (2) it controls the reaction mechanism. Condensation leads to formation of particles with sizes of 1 nm in the early stages. At pH > 7, these particles undergo a phenomena known as Ostwald ripening [7] and their average size increases to 5 - 10 nm. At low pH, growth become negligible after a size of 2 - 4 nm is reached. Vysolski et al have shown that the rate of contraction of silica at this stage has a minimum at the isoelectric point [3]. This is defined as the point where electrical mobility of the silica is zero. For silica this point is at pH

Hydrolysis and Condensation in the Sol-Gel Process.

Hydrolysis



Condensation



Polycondensation

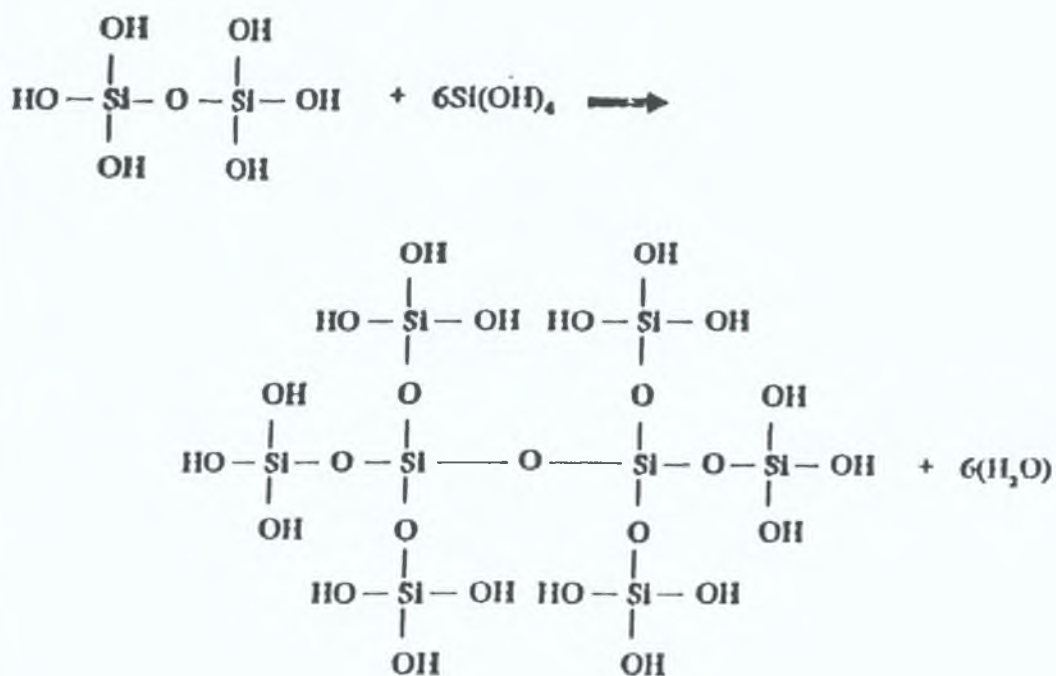


FIGURE 3.3

= 2, at which the silicate species are weakly charged, if at all. Gels prepared at a pH of 2 or lower are deemed acid catalysed, while those prepared at higher temperatures are base catalysed. Under acidic conditions ($\text{pH} < 2$), hydrolysis is rapid, and the monomers produced slowly condense by cluster-cluster growth into weakly branched polymer molecules that entangle and form a crosslinked gel. Under basic conditions ($\text{pH} > 2$), the condensation rate is much faster, and quickly consumes newly generated molecules. Such conditions favour the growth of highly branched species by monomer-cluster growth. Eventually, the highly branched clusters crosslink into a gel. These gels are referred to as "colloidal", while the former are termed "polymeric". The microstructure of polymeric gels leads to greater densification. Thus these gels will have greater bulk densities than those prepared under basic conditions. Gels prepared from basic solutions (such as those containing ammonia) show very little shrinkage and hence lower bulk densities. In general, gels with low bulk densities contain larger pores.

The type of catalyst used in the reaction can have large effects on the microstructure of the gels formed, as well as the rapidity of the gelation process. It has been found that when using H_2SO_4 instead of HCl as catalyst, bulk densities dropped by 30% and shrinkage by 5%. When HF , HCl , and H_2SO_4 were used as catalysts, gelation times went from twelve hours to ninety two hours to one hundred and six hours respectively [8].

Higher gelling temperatures (the temperature at which the sol is allowed to gel) has been found to reduce shrinkage during drying, resulting in lower bulk densities. In investigating the effects of gelling temperature on the bulk density of xerogels. It was found that increasing the gelling temperature from $54\text{ }^\circ\text{C}$ to $73\text{ }^\circ\text{C}$ reduced bulk densities by one third [9].

To avoid stress build up (which causes the gel to fracture) due to high evaporation rates, care must be taken during the drying of wet gels. The usual method is to keep the surrounding atmosphere saturated with the evaporating liquid (in this case a mixture of ethanol and water) and to allow the sol solution vapour to escape slowly through a small pinhole in the cover of the sol's container [10]. Other methods using Drying Control Chemical Additives (DCCA's) such as formamide have also been used [3]. It is the interdependence of all these factors that contributes to the difficulty of designing optimum processes for the full exploitation of sol-gel technology.

3.3 Production of Sol-Gel Thin Films

Sol-gel derived thin films have been used in a wide range of applications. These include use as antireflective coatings, solar reflective coatings, optically transparent protective coatings and optoelectronic thin films. Dye doped sol-gels have been used as laser materials and solar light guides, luminescent solar concentrators and recognition elements in chemical sensors [11]. More recently, they have been used to encapsulate the activity of enzymes and proteins [12].

The sol-gel process as applied to bulk materials has been described in detail in the last section (Section 3.2) The same chemical processes are involved in thin film production, the main differences being the shorter drying times for thin films compared to bulk materials. The following sections will describe the production of thin films using the sol-gel process; and the method of film deposition used in this project.

3.3.1 The Sol-Gel Dip Process

Several methods exist for depositing thin films. These include the relatively simple methods of Dip Coating and Spin Coating, as well as more exotic methods such as Electrochemical Polymerisation (where films are produced by the electrochemical oxidation of the monomer solution at an anode surface), and the Langmuir-Blodgett Method (where a film of reactive monomer is coated at a constant surface pressure on the substrate before photopolymerisation of the monomer) [13]. In this project a dip coating method was employed. The sol-gel dipping process is almost exclusively applied for the fabrication of optically transparent layers. It offers several significant advantages over other methods. The dipping process can be used to coat tubes, pipes, rods and fibres; and substrates of almost any size can be coated. This is of considerable importance to commercial applications since, in many instances, the economy of the process increases with substrate size.

Film thickness up to a micrometer and more can be deposited, while in this work thicknesses of approximately 300 nm were used. A high degree of film uniformity can be obtained, and thickness control is simple compared to some methods. An additional (and quite important) advantage is the ability to produce multi-layer coatings, permitting the fabrication of layers with widely varying optical characteristics.

In this study, a slight variation of the dip process was used, in that the substrate (a very clean glass slide) was held rigid while the vessel containing the sol was lowered. During the dipping process, the polymers are concentrated and sheared as the solvent flows and evaporates from the substrate surface. The polymers continue to condense as unreacted terminal groups come into contact. Condensation reactions take place both within and between the polymer chains and the substrate. Depending

on the relative rates of shear, condensation and evaporation, as well as the surface tension of the solvent, gelation may occur at an early or late stage of the drying process. As mentioned in Section 3.3, compared to bulk gels, drying occurs very rapidly for thin films resulting, generally, in higher densities and reduced porosities. Porosity of films can be optimised by aging the sol prior to dipping. This enables aggregation of sol particles by condensation reactions, thus giving rise to less dense, more porous films [14].

The film is constrained in the plane of the substrate and thus shrinkage occurs in the direction normal to the substrate surface. This imposes tensile stress in the plane of the film, which can retard film consolidation and lead to cracking.

The deposition method influences the film structure. Dipped films will often be less dense than the corresponding spun films. This is a consequence of the increased rate of evaporation that occurs during spinning. Depending on the application of the final product, film thickness can be of extreme importance. Thickness is controlled by both intrinsic and extrinsic factors. Example of extrinsic factors include viscosity, surface tension and vapour pressure. When dipping, film thickness is further affected by the speed of withdrawal and angle of inclination of the substrate surface to liquid interface. The thickness of spun films depends on spin speed.

It is clear that, as well as all the factors that must be considered with regard to sol preparation, the above points must also be taken into account when producing thin films from sol-gels.

The next chapter describes how the dipping process was carried out, and includes a diagram of the apparatus used to coat samples.

3.4 Summary

Sol-gel and conventional glasses were compared and some of the advantages offered by sol-gel derived glasses were discussed. The sol-gel process was described in detail, including the effects of changing various parameters (such as solution pH, type of catalyst, and gelling temperature) on the final product. The production of thin films using the sol-gel process was also discussed.

This project will investigate the feasibility of an oxygen sensor based on the fluorescence quenching of ruthenium complexes incorporated into a silica sol-gel thin film. In principle, a porous sol-gel should be an ideal sensor support. The sol-gel technique facilitates coating of planar and optical fibre substrates, and the method allows tailoring of the film properties.

References:

- [1] "Concise Encyclopedia of Science and Technology"; edited by John David Yale. Published by Phaidon Press Ltd., 1978.
- [2] "A structural study of the Sol-gel process by optical fluorescence and decay time spectroscopy"; K. Devlin, B. O'Kelly, Z.R. Tang, C. McDonagh, J. McGilp; *Journal of Non Crystalline Solids*, Vol. 135, 1991, pp 8-14.
- [3] "The Sol-gel process"; L. Hench and J. West; *Chemical Review*, Vol. 90, pp 33-72, 1990.
- [4] "The Production and Optical Investigation of Ion-Doped Sol-Gel derived Silica"; P. Marron. From M.Sc. Thesis: "The production and optical investigation of ion-doped sol-gel-derived silica." presented to Dublin City University 1993 (unpublished).
- [5] "Structural Investigation of Sol-gel silica using optical probes"; C. McDonagh, G. Ennis, P. Marron; *Journal of Non Crystalline Solids*, Vol. 147, 1992, pp 97-101.
- [6] "Sol-gel processes in Glass science and technology"; S.P. Mukherjee. *Journal of Non Crystalline Solids*, Vol. 42, 1980, pp 477-488.
- [7] "The Gel to Glass Transition: Chemical and Microstructural Evolution"; P. F. James, *Journal of Non Crystalline Solids*, Vol. 100, 1988, pp 93-114.

- [8] "Applications of the Sol-gel method: some aspects of initial processing, J.D. Mackenzie; from "The Science of Ceramic Chemical Processing" edited by L. Hench and D. Ulrich. Published by Wiley, 1986.
- [9] "Monolith formation from the Sol-gel process"; M. Yamane from "Sol-gel technology for thin films, fibers, preforms, electronics and speciality shapes" compiled by L. Klein.
- [10] "Effects of Temperature on the formation of Silica gels"; C. Colby, Y. Osaka, J.D Mackenzie; Journal of Non Crystalline Solids, Vol. 199, 1990.
- [11] "Characterisation of Rhodamine 6G-doped thin Sol-gel films"; U. Narang, F. Bright, P. Prasad. Applied Spectroscopy, Vol. 47, No. 2, pp 229-233, 1993.
- [12] "Organic fluorescent dyes trapped in Silica and Silica-Titania films by the Sol-gel method"; D. Avnir, V. Kaufman, R. Reisfeld; Journal of Non Crystalline Solids, Vol. 74, pp 395-406, 1985.
- [13] "Design, Ultrastructure and Dynamics of polymeric thin films"; P. Prasad; from "The Science of Ceramic Chemical processing" by Hench and Ulrich, Chapter 46 Published by Wiley, 1986.
- [14] "Sol-Gel Science", edited by C. Brinker and G. Scherer. Published Academic Press (New York) 1989.

Chapter 4

Experimental

4.0 Introduction

The experimental systems used in this work are described in this chapter. Sol preparation, sample coating and set-up, and the two different procedures used to make Fluorescent Intensity and Fluorescent Decay time (or lifetime) measurements are also discussed.

4.1 Sol preparation

Significant care must be taken when preparing the sol to ensure the uniformity of the final coatings. The apparatus used must be clean, not only to avoid general contamination, but also because polymeric reactions are involved. (Unwanted polymerisation and precipitation can occur on the surface of small foreign particles).

The sols were prepared as follows:

For a pre-doped sol, the appropriate amount of dopant was weighed into a clean glass vial.

To this was added the correct amount of water ($\text{pH} = 1$) and ethanol, and the solution lightly stirred.

To this solution, tetraethylorthosilicate (TEOS) was added dropwise with vigorous stirring as TEOS and water are only very slightly miscible. If the TEOS is added too quickly, the solution will become cloudy, although it will clear again after sufficient

stirring. The resultant solution was stirred for at least 20 minutes and stood to age before substrate dipping. During this aging process, the hydrolysis and condensation reactions continue, and the formation of porosity occurs. An aged solution is more suitable for dipping as it becomes more adhesive, and will bond better to a substrate. Ageing periods ranged from 24 hours when aged at room temperature down to 14 hours when aged at 73°C.

4.1.1 Substrate coating

To facilitate both planar and fibre optic substrates, it was decided that a dip-coating method would be employed. The dip-coater constructed for this purpose is shown in Figure 4.1. The solution reservoir is clamped on to a moveable platform. A computer controlled stepper-motor turns a screw which raises or lowers this platform. The substrate to be coated is held rigidly normal to the surface of the liquid, while the sol reservoir is lowered. The speed at which the reservoir is lowered, i.e the effective withdrawal speed of the substrate is controlled by computer. This method ensures uniform dipping speed, this is very important since dipping speed has a huge influence on film thickness. (See Section 3.4.1). This technique proved to give smooth coatings of very good quality when examined under a microscope.

Immediately after dipping, the coated substrates are placed in an oven at 73°C and left to dry for at least 24 hours. This low temperature thermal processing results in a thin film of xerogel coating on the substrate.

4.1.2 Thin film fabrication

Depending on the desired final characteristics of a sol-gel derived glass, certain parameters in its composition can be varied. These factors include the molar ratio,

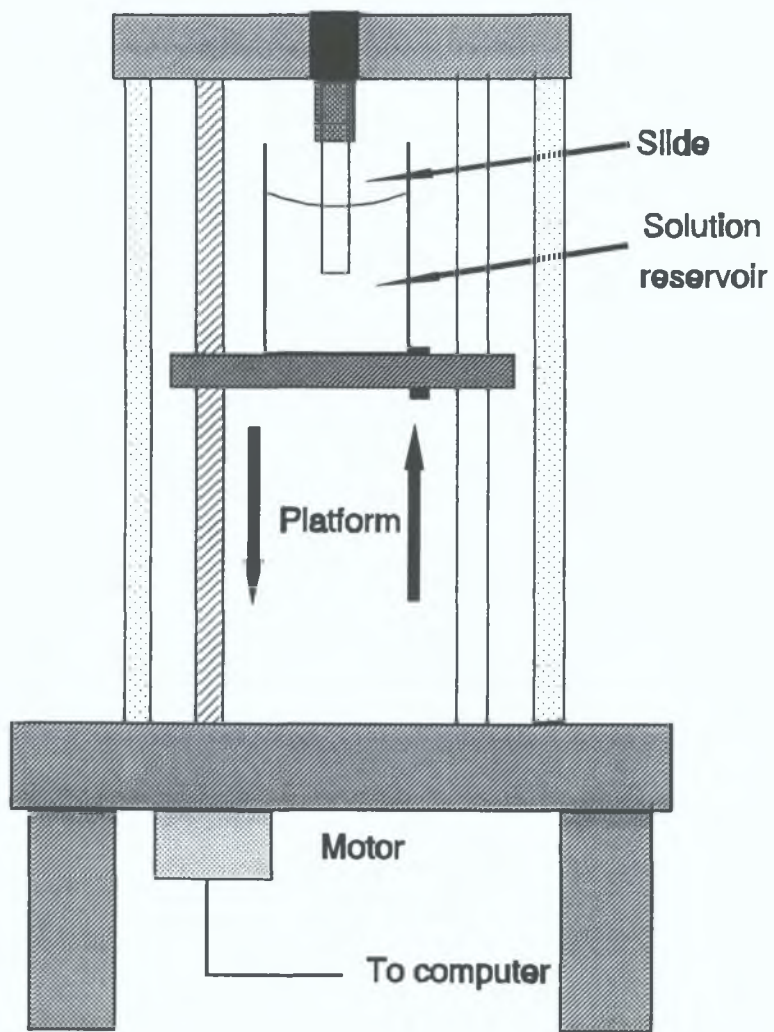


Figure 4.1
Dip-coating apparatus

r, of water to TEOS, solution pH, treatment of the sol after mixing. When fabricating thin films, dip speed must also be taken into account.

4.1.3 Water to TEOS ratio, r

The minimum number of moles of water per mole of TEOS required for complete hydrolysis is 2 [1]. If less than 2 moles of water per mole of TEOS are present, a fraction of the TEOS will remain unreacted and polycondensation will cease. It was found that a ratio of 2 : 1 produced good quality films, and this ratio was used throughout the project.

4.1.4 Solution pH

The starting pH of the solution mixture plays a major role in the final structure of the gel. Solution pH was varied from pH of 1 to 3 to 5.

Films made at pH = 3 and pH = 5 were cloudy in appearance, due to the large size of the pores formed at these pH values, and tended to bond very poorly to the cleaned glass substrate. Those made at pH = 1 gave smooth, transparent, crack-free coatings that adhered excellently to the substrate. These coatings proved to be very durable with no significant loss in sensing performance over a time period of 5 months.

4.1.5 Sol treatment prior to dipping

After mixing, the sols were left to stand, or age, before dipping. This allows the sols to begin to polymerise ensuring a better bond to the substrate.

The solutions were stood in air in glass containers (with a small pinhole in the lid to allow for the escape of solution vapour). The sols were aged at one of two

temperatures, room temperature (approximately 25°C), or at 73°C. Ageing times were 24 hours and 14 hours respectively. Sols aged at 73°C for more than 17 hours polymerised fully to gels and thus were of no use for dipping purposes.

The sensing performance of films made from sols aged at the two different temperatures is compared in Chapter 5.

4.1.6 Film deposition

If films are produced by a dip-coating technique, the film thickness will depend, amongst other things, on dip speed.

For fluorophore-doped thin films, it is desirable to have a relatively thick coating so that the absolute fluorescent intensity from the coated substrate is high (due to the greater number of fluorescent molecules present). However if the film is too thick, then cracking will occur during the drying stage.

In this case, the glass substrate onto which the coating is to be deposited is held rigid, and the sol reservoir lowered. Thus it is the rate at which the reservoir is lowered that determined film thickness.

The dip coater constructed allowed for withdrawal rates up to 3 mm/s. Substrates were dipped at speeds from 0.2 mm/s to 1.5 mm/s.

Films produced at the lower speed were very thin, and for reasonable fluorophore concentrations, gave very low absolute intensity signals. Best results were obtained with a dip speed of 1mm/s. This gave crack-free coatings of approximately 300 nm in thickness.

4.1.7 Film drying

Low temperature thermal treatment of the coated substrates is necessary to ensure complete gelation of the films.

Immediately after dipping, the substrates were held vertically in an oven to dry at 73°C for at least 24 hours. Due to the dry environment of the oven, most of the reaction solvents are removed at this stage. It was observed that once dried for 24 hours at 73°C, further drying at this temperature had no effect on sensor performance.

4.2 Fluorescent Species and Concentration

4.2.1 Choice of fluorescent species

The two fluorescent species used in this project were $\text{Ru}(\text{bpy})_3^{++}$ and $\text{Ru}(\text{Ph}_2\text{phen})_3^{++}$. Each compound was impregnated into similar sol-gel thin films, and the behaviour of the fluorescent intensity and lifetime of each in the presence of oxygen was examined.

4.2.2 Fluorescent species concentration

The concentration of the fluorescent species in the sol-gel matrix is important. It is desirable to have a concentration high enough so that there is a strong fluorescent signal from the coating. If concentrations are too high however, a phenomenon known as concentration quenching can occur. This is a form of non-radiative relaxation caused by the absorption of fluorescent radiation by other fluorophore molecules within the matrix.

Coatings were prepared with fluorophore concentrations of 10000, 20000, 40000, and

80000 ppm, and the performance of each compared. (Note: 1 ppm means 1 part fluorophore to 1000000 part solution)

4.3 Sample setup

The samples were mounted in a gas cell (see Figure 4.2), which allowed the introduction of a preset oxygen/nitrogen gas mixture. Nitrogen has no effect on the fluorescent properties of the compounds used, so 100% nitrogen was deemed to be 0% oxygen, 90% nitrogen/10% oxygen to be 10% oxygen etc. The oxygen concentration of the gas mixture was determined by mixing the two gases in the desired ratios using Unit Instruments mass flow controllers (M.F.C's) and a URS100 Mixing unit.

The gas mixture was allowed to flow through the gas cell for several minutes to ensure correct oxygen/nitrogen concentrations, and a homogenous gas mixture.

4.4 Fluorescent Intensity Measurements

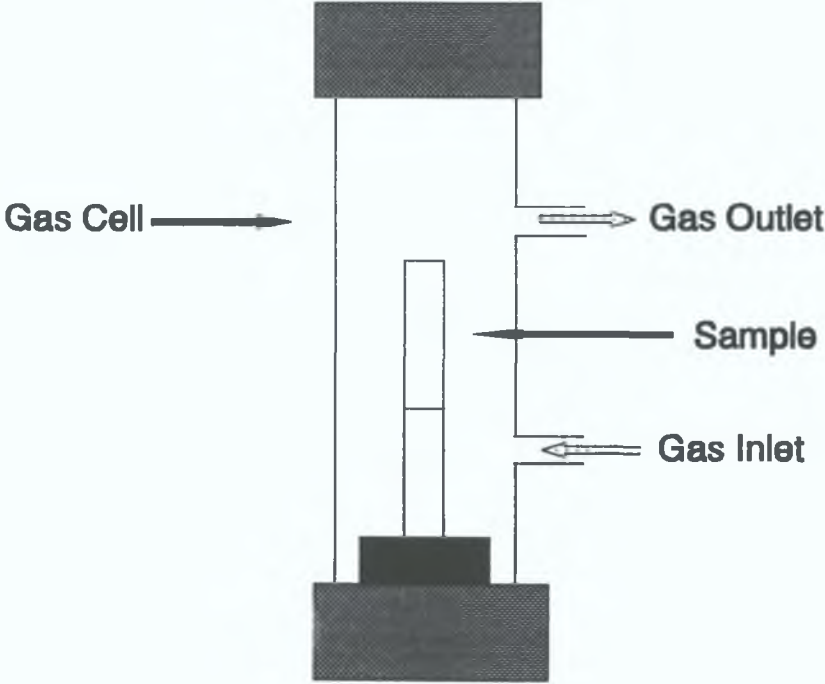
The experimental setup is shown in Figure 4.3.

Two excitation sources were used. The first was a 200 W Applied Photophysics water-cooled Xe arc lamp. Light at a wavelength of 460 nm, (the maximum absorption peak for the ruthenium compounds), was selected by passing the lamp output through a monochromator.

A more convenient and efficient excitation source, an Omnichrome Model 532-200MA Argon ion laser ($\lambda_{\text{ex}} = 488 \text{ nm}$), was chosen as it had superior stability and power output. As can be seen from the Figure 4.3, the excitation source and spectrometer are at right angles to each other, which minimises scattering of excitation radiation at the detector.

Figure 4.2

Gas Cell



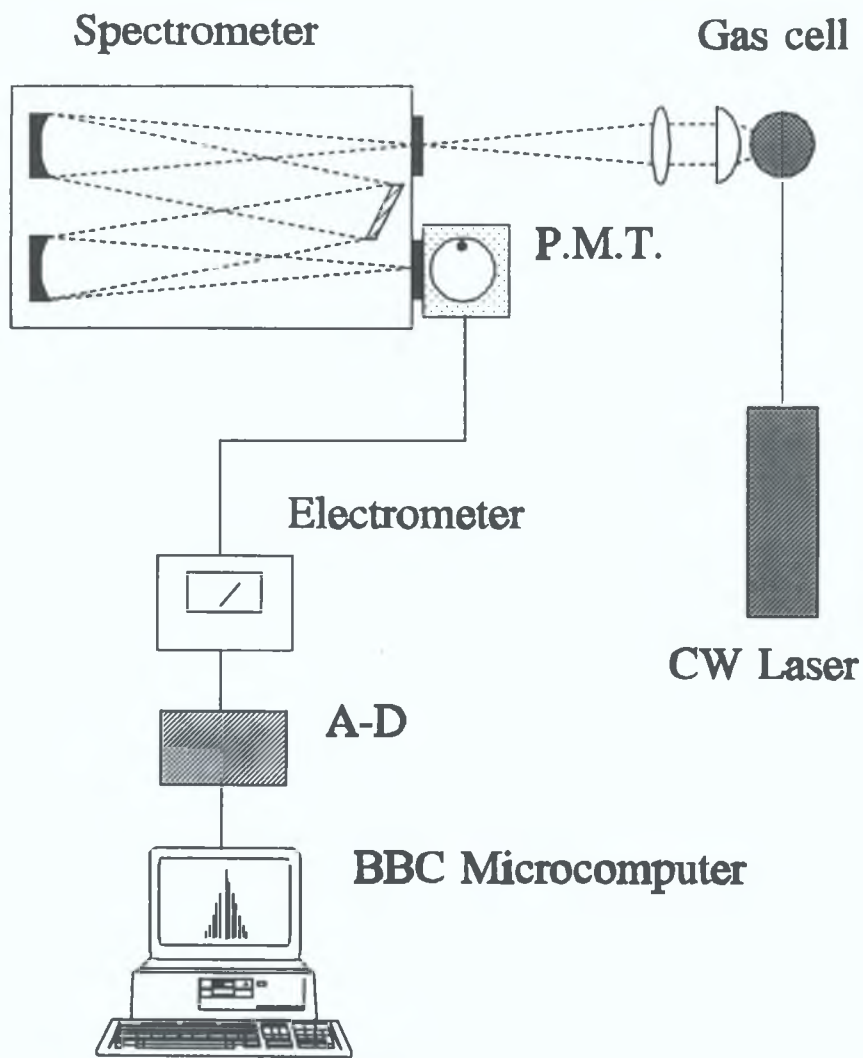


Figure 4.3
Intensity measurement setup

The fluorescence from the sample was collected and focused onto the slit of a Jobin Yvon 1m focal length spectrometer (set at 615 nm), and detected by a Hamamatsu R928 photomultiplier tube (P.M.T.) To prevent any interference from scattered excitation radiation, filters which selected a narrow wavelength band centred at 610nm were placed over the slit of the spectrometer.

4.4.1 Data Acquisition

The signal from the P.M.T. was fed to a BBC Master Series microcomputer via an electrometer and an Acorn Electronics Analogue interface board. The BBC microcomputer was used to record plots of fluorescent intensity versus oxygen concentration, and by allowing the spectrometer to scan across different wavelengths, to obtain fluorescent intensity versus wavelength plots.

Time averaging of the signal was achieved by the BBC microcomputer through sampling each data point. Background (or ambient count) subtraction was also carried out by the computer.

4.5 Lifetime Measurements

The experimental setup is shown in Figure 4.4

The source used was a Spectron Laser Systems Nd-Yag pulsed laser, frequency doubled to 532 nm. Although this is towards the end of the Ruthenia complexes' absorption bands, the ample light intensity from the laser ensured a very strong fluorescent signal. The laser was set to deliver a 50 ns pulse at a repetition rate of 15 Hz. To avoid photobleaching of the samples, neutral density filters were used to cut down the intensity of the excitation radiation. The fluorescent radiation was gathered as before, passed through a filter (to remove any scattered excitation

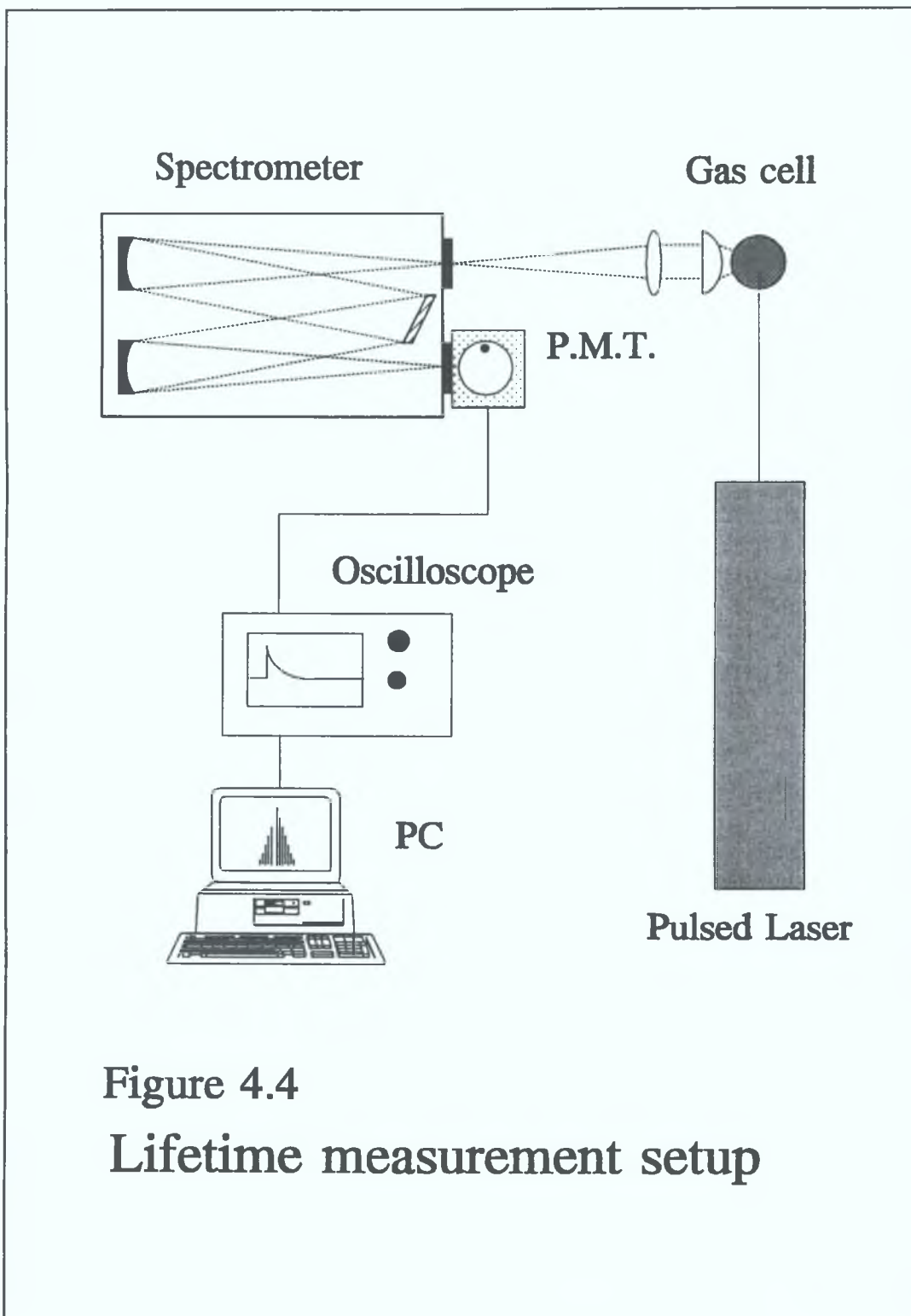


Figure 4.4
Lifetime measurement setup

radiation) and spectrometer to the P.M.T. The signal from the P.M.T. was fed into a Hewlett-Packard 54600A digital storage scope (input impedance 50 Ohms), whose output was connected to an IBM compatible PC.

4.5.1 Data Acquisition

The oscilloscope allowed signal averaging and storage. The signal is stored as a series of two data columns, one represents the "Time" or X-axis, the other represents the "Voltage" or Y-axis. These data columns (representing the decay of the fluorescent radiation with time) were downloaded (via an RS-232 cable) to PC using the commercial software package SCOPELINK.

The data was then converted to Apple Mac form (using 'Apple File translator) in order to allow processing with the powerful 'Kaleidagraph' software package.

4.6 Fluorescent Lifetime Calculation.

In an ideal situation, the fluorescent lifetime Of a fluorophore will follow a single exponential decay. When an optically active fluorophore is first excited, it emits a maximum intensity I_0 . The rate at which this intensity decreases with time is characterised by the lifetime, τ , of the excited state. The time dependence of the decay is described by the following equation:

$$I = I_0 \cdot e^{-Kt} \quad \text{Eqn...1}$$

where K is the decay rate constant. (Note $K = \tau^{-1}$).

Hence, the lifetime of the excited state can be measured as the time taken for the emitted radiation to fall to 1/e of its original intensity. The above equation can be rewritten as:

$$\ln I = \ln I_0 - Kt \quad \text{Eqn...2}$$

indicating that a semi-logarithmic plot of $\ln I$ versus t will have a slope of $-K$, from which the lifetime is easily calculated [2] .

Figure 4.6 (a) shows the decay of a 10^{-3} Molar solution of $\text{Ru}(\text{Ph}_2\text{phen})_3^{++}$ in ethanol, through which nitrogen gas has been bubbled for 10 minutes. This ensures the removal of any dissolved oxygen, and hence a complete absence of the quenching species. This situation is very close to being ideal.

The Kaleidagraph package used has a curve fitting option which allows the user to fit exponential curves to data. If a decay is a single exponential, then the exponential curve fit will match the decay exactly. Figure 4.6 (a) also shows a single exponential curve fitted to the decay curve. This curve fit fits very well, and has a correlation coefficient close to 1.

Figure 4.6 (b) shows the fluorescent decay of the same solution under 100 % oxygen on the same scale as Figure 4.6(a). As can be seen, there is a large change in the lifetime of the fluorophore. Figure 4.6 (c) has a time scale one tenth of those in Figures 4.6 (a) and (b), and on this scale we can see that the decay still follows a single exponential. Figures 4.6 (d) and (e) show semi-logarithmic plots of the same data. Straight lines are achieved for both graphs, and from their slopes, the lifetimes in 0% and 100% oxygen are 4.3 μs and 350 ns respectively.

The sol-gel support matrices are not 100% porous however, and so trapped within the thin film coatings there will in effect exist (at least) two "types" of fluorescent sites, one accessible and one inaccessible to oxygen. This will give at least two components in the lifetime decay. This can complicate lifetime calculations.

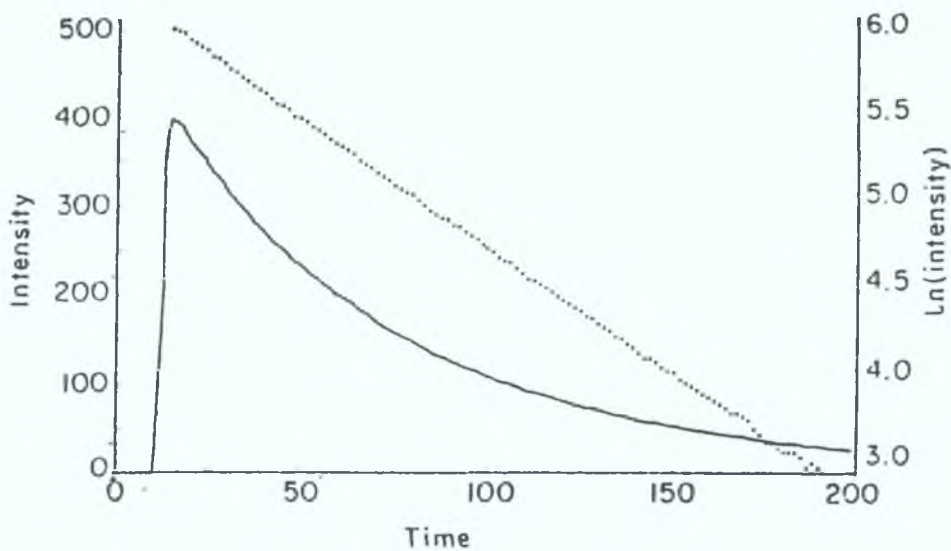
For the case of a two-component decay, two methods of lifetime analysis were investigated: (a) Line Stripping technique and (b) Numerical Integration of the area

under the lifetime curve (which changes with oxygen concentration).

4.6.1 Line stripping

The majority of lifetime measurements involve first order decay processes. According to Equations 1 and 2 in Section 4.6, a first order decay will have a profile similar to that below. The dashed line is a semilogarithmic plot of $[I]$ versus time.

Figure 4.6.1 (a)



However, a problem arises when the decay is not first order. This can occur when several species with different lifetimes emit simultaneously and independently. Although such systems usually arise from impure samples or mixtures, they can also occur in pure samples containing different fluorescing sites.

In the above cases, a multicomponent decay will be observed. In general, semilogarithmic plots of $[I]$ versus time are concave upward for multicomponent systems. If only two components are present, and their lifetimes are sufficiently

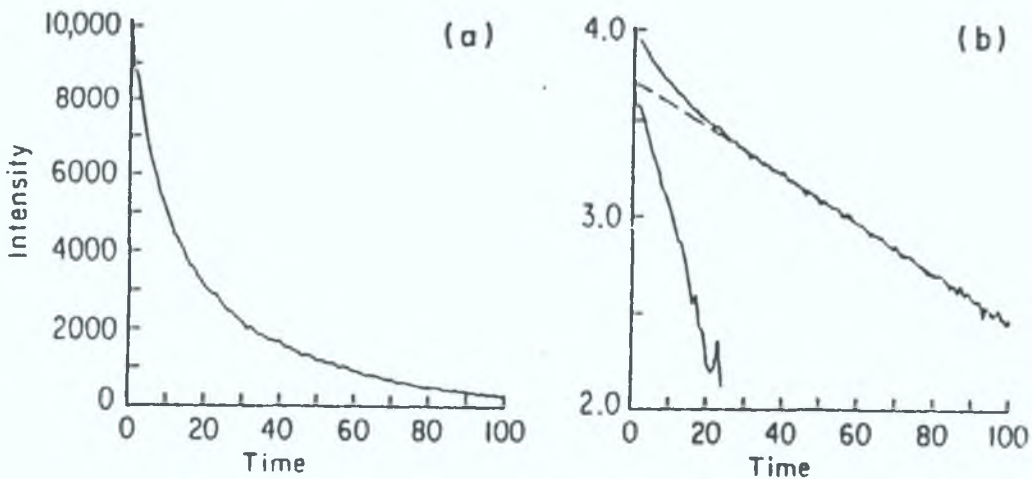
different, then the lifetimes can be resolved by line stripping techniques [2] .

Consider Figures 4.6.1 (b) and (c), which show a two component lifetime decay and semilogarithmic plot of this decay respectively. At long enough times, the semilogarithmic curve will be linear, and from this a lifetime, τ_{slow} , for the slow component. The contribution of the slow component can then be subtracted from the original decay, [I] to yield:

$$[I]_{fast} = [I]_{orig.} - I_{slow} \cdot e^{-(t/\tau_{slow})} \quad \text{Eqn...3}$$

[I]fast approximates the pure decay curve for the short lived component, and from this the short component lifetime can be calculated.

Figures 4.6.1 (b) and (c).



4.6.2 Numerical Integration

Another, more straightforward, method of analysing complicated decay curves can also be employed. The average lifetime, τ_{avg} can be defined as:

$$\tau_{avg} = \frac{\int t I(t) dt}{\int I(t) dt} \quad \text{Eqn...4}$$

where I(t) is the experimental decay curve [2] .

When using this method, the area under the lifetime curve is used to analyse the

Figure 4.6 (a)

10^{-4} Molar $\text{Ru}(\text{Ph}_2\text{phen})_3^{++}$ solution
in 100% Nitrogen.

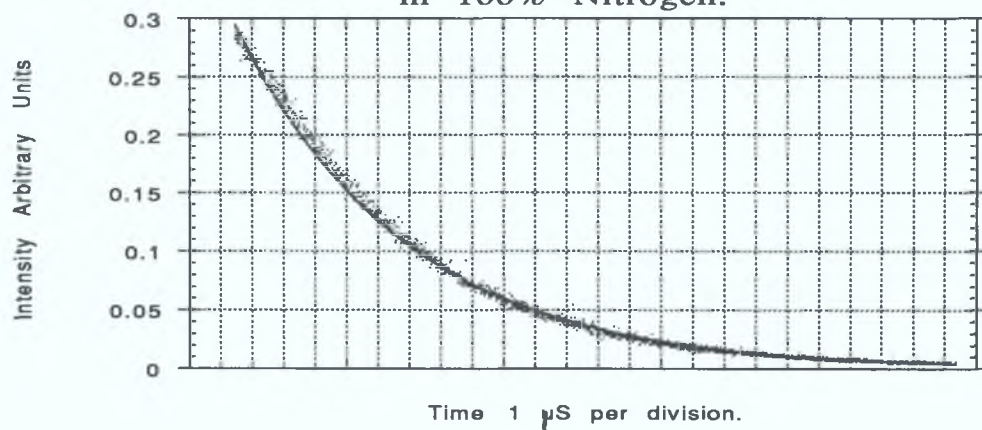


Figure 4.6 (b)

10^{-4} $\text{Ru}(\text{Ph}_2\text{phen})_3^{++}$ solution
in 100% Oxygen.

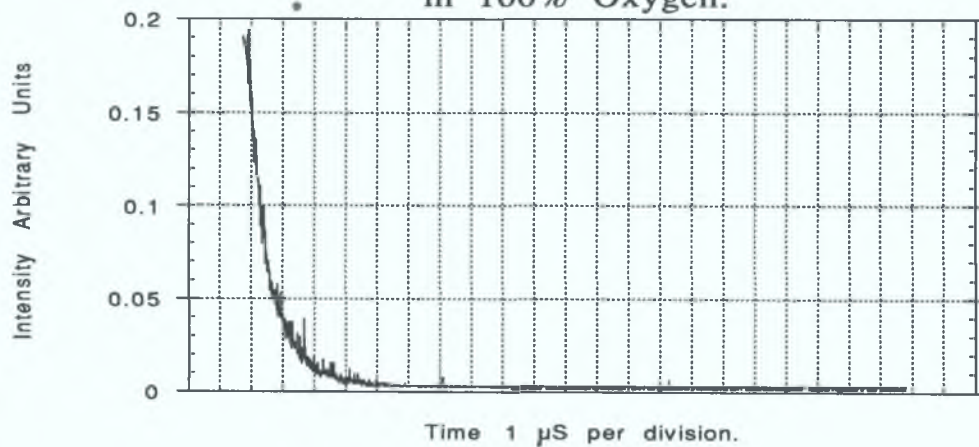


Figure 4.6 (c)

10^{-4} $\text{Ru}(\text{Ph}_2\text{phen})_3^{++}$ solution
in 100% Oxygen.

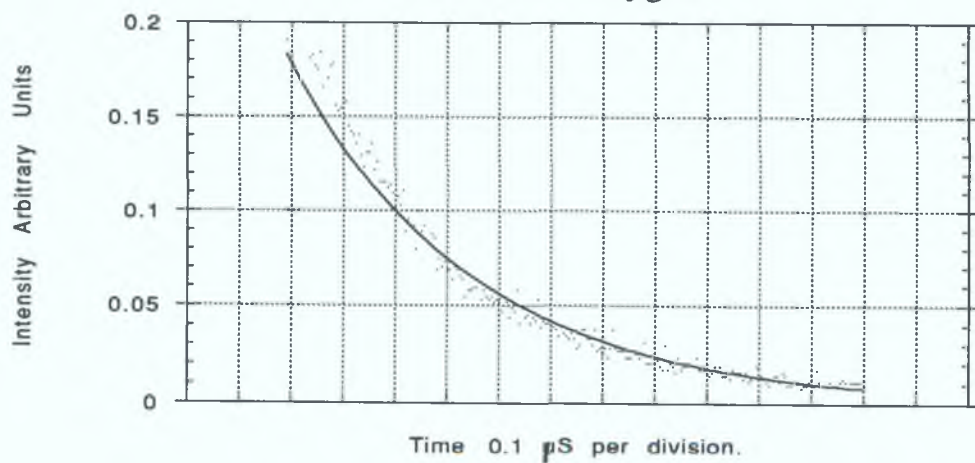
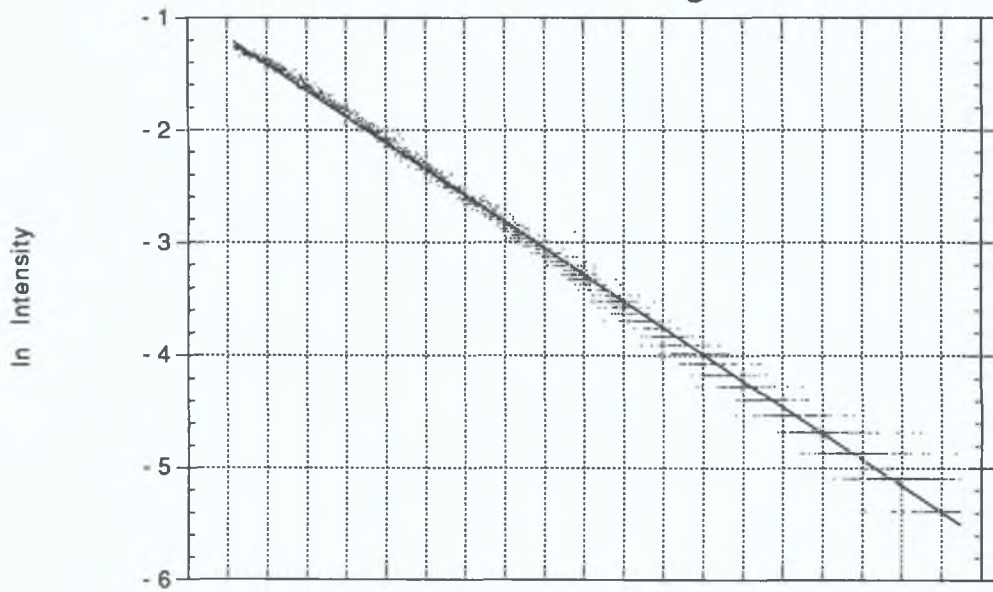


Figure 4.6 (d)

10^{-4} Molar $\text{Ru}(\text{Ph}_2\text{phen})_3^{++}$ solution
in 100% Nitrogen



Time 1 μS per division.

Figure 4.6 (e)

10^{-4} Molar $\text{Ru}(\text{Ph}_2\text{phen})_3^{++}$ solution
in 100% Oxygen.



Time 1 μS per division.

Figure 4.6.2 (a) Typical Decay under 100% Nitrogen
for 20000ppm $\text{Ru}(\text{Ph}_2\text{phen})_3^{++}$ sample.

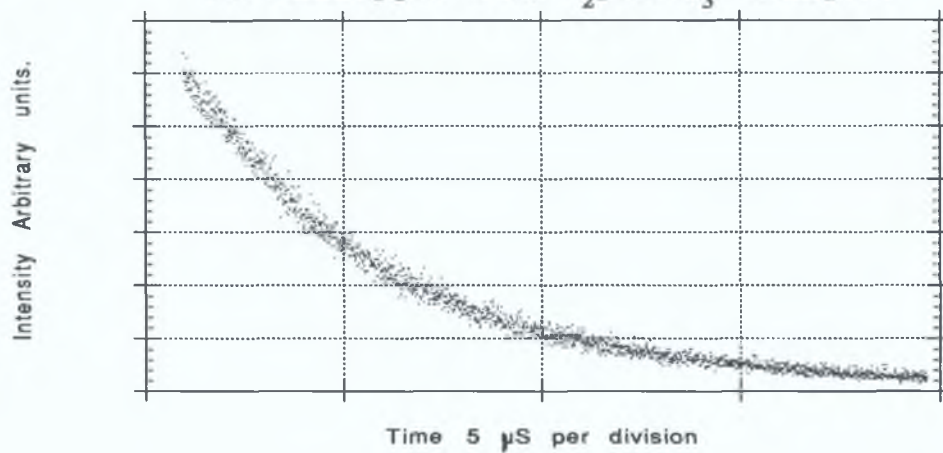


Figure 4.6.2 (b) Typical Decay under intermediate
Oxygen concentration.

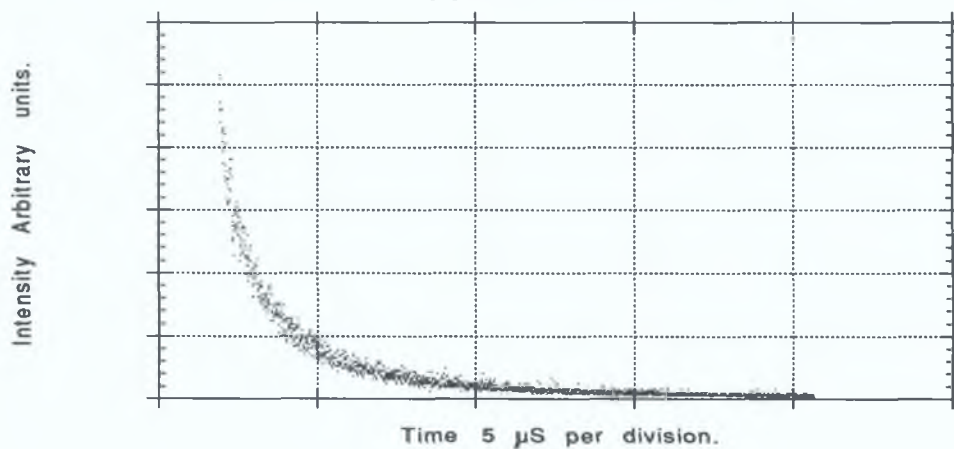
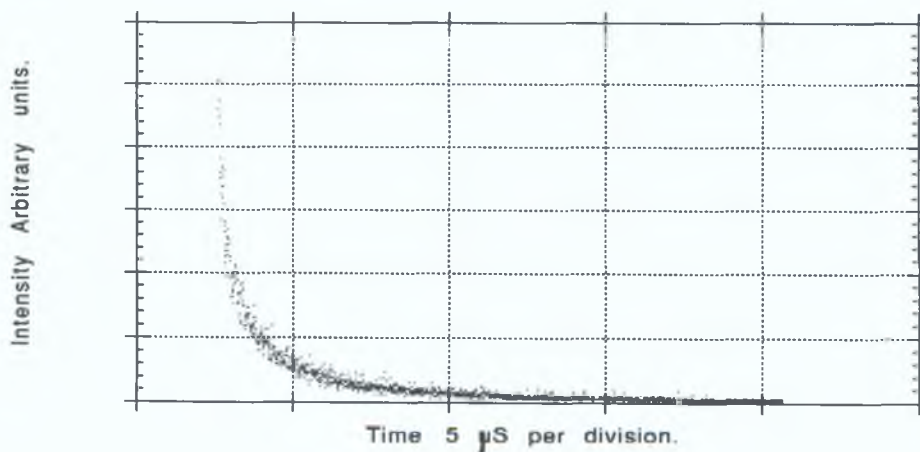


Figure 4.6.2 (c) Typical Decay under 100% Oxygen.



lifetime. The area under the curve decreases with increasing quencher concentration. Figures 4.6.2 (a), (b), and (c) show how the area changes for a typical sample for oxygen concentrations between 0 and 100%. Using a computer, the area under the curve can be calculated and thus related to quencher concentration.

4.7 Summary

Chapter 4 described the fabrication of ruthenium complex doped thin sol-gel films. Great care was taken to deposit consistent, uniform films on the substrates after the parameters such as solution pH etc. were optimised. Prior to dipping the films were subjected to two different aging temperatures, and films were dipped at different speeds in order to obtain clear, long lasting coatings. The coatings were doped with two different complexes, $\text{Ru}(\text{bpy})_3^{++}$ and $\text{Ru}(\text{Ph}_2\text{phen})_3^{++}$, with varying concentrations of both. The experimental systems used to examine the change in fluorescent intensity and lifetime of the two complexes were described in detail, in particular calculation of the fluorescent lifetime which involved two methods.

The next chapter discusses the results obtained, including the performance of each dye, and dye concentration when exposed to oxygen.

References:

- [1] "The Sol-gel process"; L. Hench and J. West; Chemical Review, Vol. 90, pp 33-72, 1990.
- [2] "Excited state lifetime measurements "; J.N.Demas, academic press, New york 1983.

Chapter 5

Results

5.0 Introduction

Samples containing $\text{Ru}(\text{bpy})_3^{++}$ and $\text{Ru}(\text{Ph}_2\text{phen})_3^{++}$ were examined using the techniques described in the previous chapter. The change in both fluorescent intensity and lifetime with changing oxygen concentration is compared and contrasted, as well as the methods used to calculate the lifetime. Different samples were analysed to determine the optimum dye concentration, sol treatment and long term performance.

5.1 $\text{Ru}(\text{bpy})_3^{++}$

5.1.1 Optimum dye concentration

It is important that an optimum concentration of fluorescent species within the sol-gel matrix be established. When dealing with doped films of approximately 300nm in thickness, the fluorophore concentration must be high enough to give a strong, easily detected fluorescent signal. If the concentration is too high, however, concentration quenching can occur (see section 4.2.2).

Figure 5.1.1(a) is a graph of fluorescent intensity versus oxygen concentration for samples with $\text{Ru}(\text{bpy})_3^{++}$ concentrations between 20000ppm and 80000ppm. There is clearly a concentration quenching effect in that the 80000ppm intensity is lower. However as shown in figure 5.1.1(b) the Stern-Volmer plot of the above data indicate a slightly better response for the 80000ppm sample. Hence this was the dye concentration used for the remainder of the study.

Figure 5.1.1 (a)

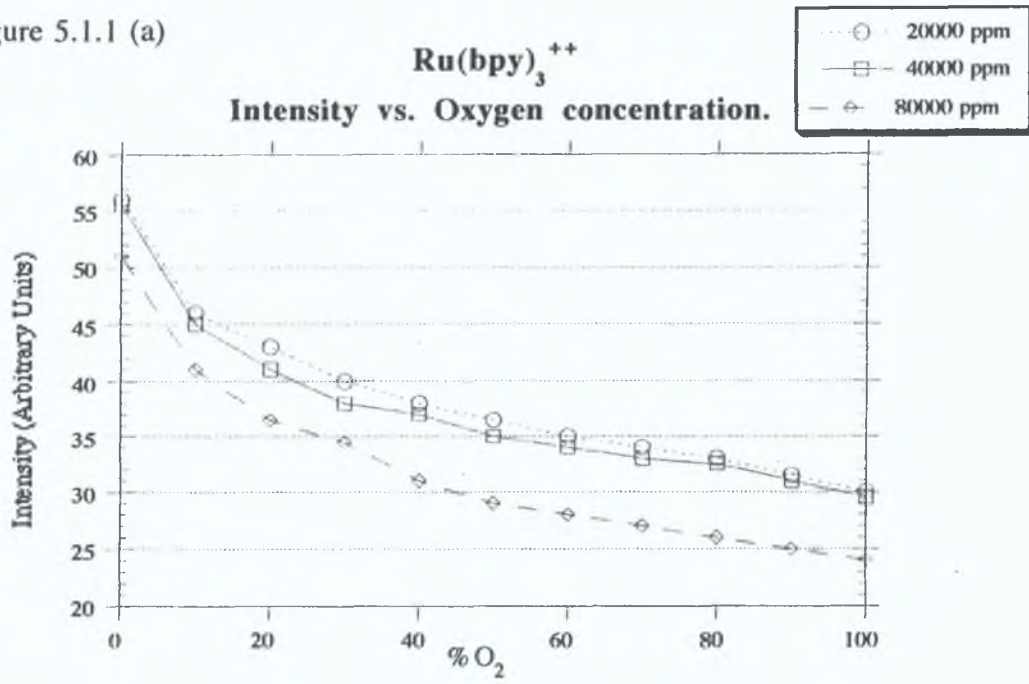
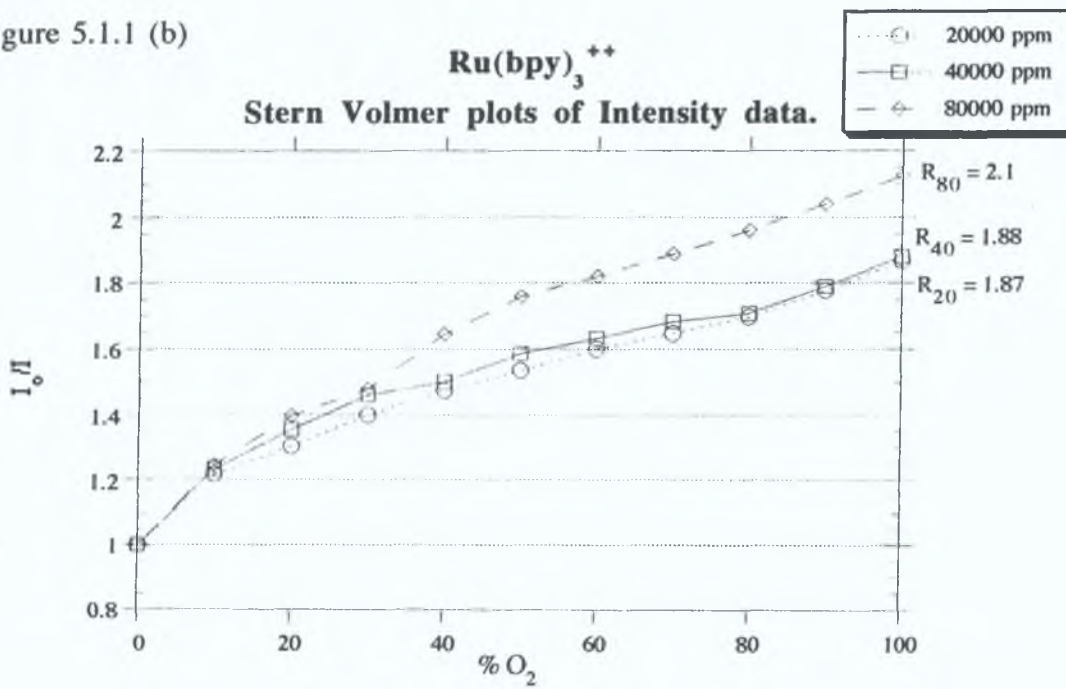


Figure 5.1.1 (b)



5.1.2 Fluorescent Intensity vs. Oxygen concentration

Figure 5.1.2(a) shows how the absolute fluorescent intensity from a typical 80000ppm $\text{Ru}(\text{bpy})_3^{++}$ doped sample changes from a maximum in the absence of oxygen to a minimum under 100% oxygen. Under 100% oxygen the fluorescent signal is reduced to just under 48% of its value in the absence of quencher. The performance of the same sample over an oxygen concentration range of 0-100% is shown in Figure 5.1.2(b), and the corresponding Stern-Volmer plot in Figure 5.1.2(c). This graph has a R value of 2.1. The R value is the ratio of the fluorescent intensity (or lifetime) in the complete absence of quencher to the value of fluorescent intensity (or lifetime) under 100% quencher concentration.

Although this R value of 2.1 is reasonable, a greater response to oxygen would be desirable for sensing applications.

Figure 5.1.2 (a) 80000ppm $\text{Ru}(\text{bpy})_3^{++}$ sample: Change in Absolute Intensity between 0% and 100% Oxygen concentration.

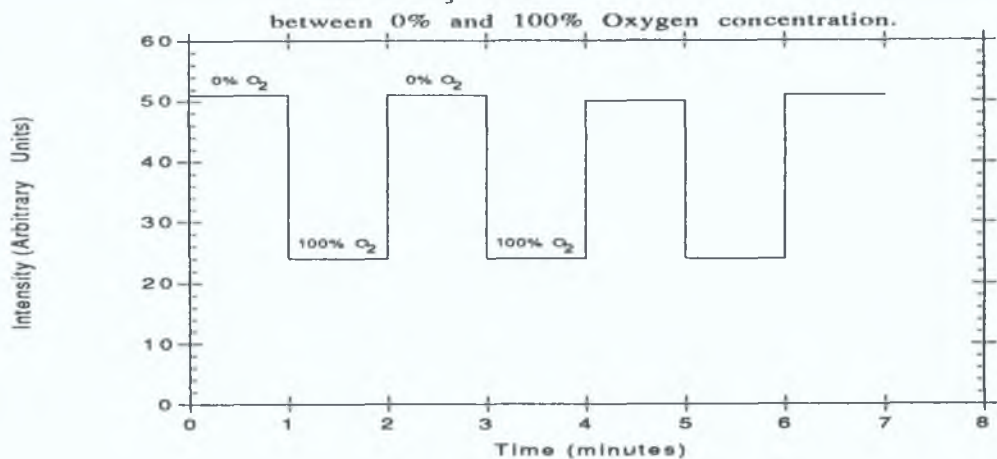


Figure 5.1.2 (b) 80000ppm $\text{Ru}(\text{bpy})_3^{++}$ sample: Intensity vs. Oxygen concentration.

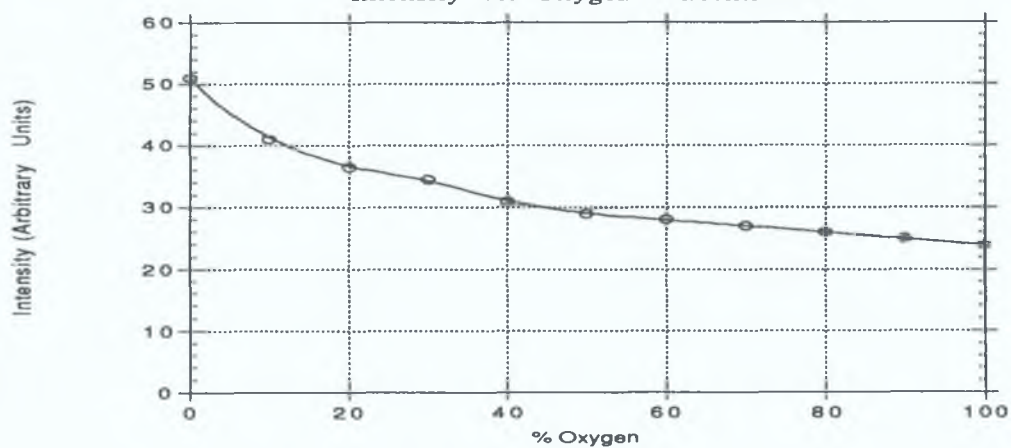
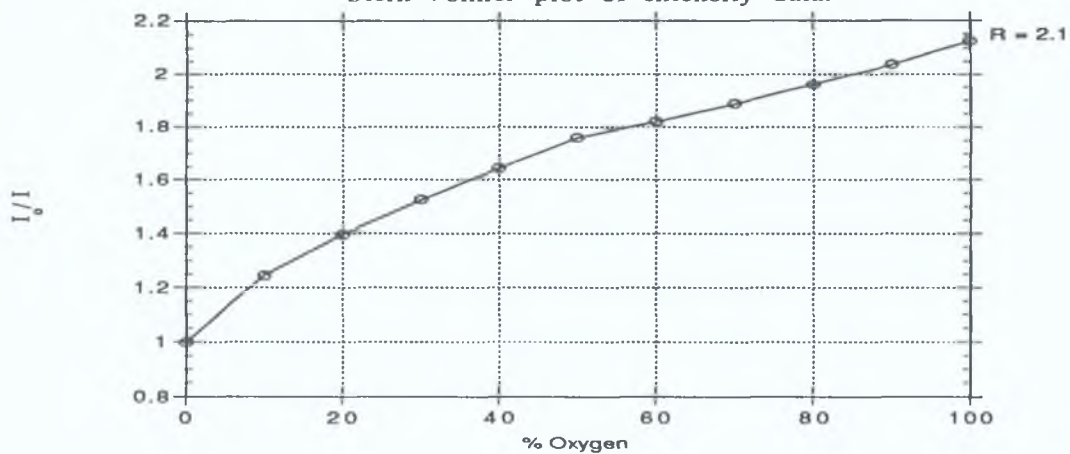


Figure 5.1.2 (c) 80000ppm $\text{Ru}(\text{bpy})_3^{++}$ sample: Stern-Volmer plot of Intensity data.



5.1.3 Fluorescent Lifetime vs. Oxygen concentration

The fluorescent lifetime of the dyes investigated were measured using two techniques, viz. "Line Stripping" and "Numerical Integration". As discussed in Chapter 4, due to the fact that the sol-gel matrix is not 100% porous, there will exist within the thin film coatings (at least) two types of fluorescent sites. One will be accessible to quenching by oxygen. The other, trapped in the non-porous areas of the matrix, remains inaccessible to oxygen. This will result in multiexponential decays. If a homogenous quenching environment is assumed, then in the complete absence of oxygen, the lifetime should follow the same exponential decay for the fluorophores both accessible and inaccessible to oxygen. Under 100% oxygen, a two component decay will be observed; a rapid quenched component superimposed on a slower unquenched decay (due the fraction of inaccessible fluorophores).

The fluorescent decay of each sample was recorded on a digital storage oscilloscope and the resultant data examined with the Kaleidagraph™ package for Apple Macintosh™ computers

Figure 5.1.3 (a) shows the decay of a typical sample under 20% oxygen. This decay is the sum of at least two exponentials as discussed above, one a fast decay, the other much slower. Using the curve fitting technique a curve was fitted to the end portion of the decay, where it can be certain that the rapid quenched decay has ceased. Kaleidagraph can display an equation for this portion of the decay, from which a "slow" lifetime can be evaluated. Optimum curve fits were obtained by optimising the correlation coefficient, of the fit. Data was generated from this equation and this new, "slow" decay can be displayed on screen as in Figure 5.1.3 (b). This data can be subtracted from the original curve data, resulting in a new "fast" or stripped decay curve as in Figure 5.1.3 (c). When a curve is fitted to this

Figure 5.1.3 (a)

Fluorescent Decay under 20% Oxygen.

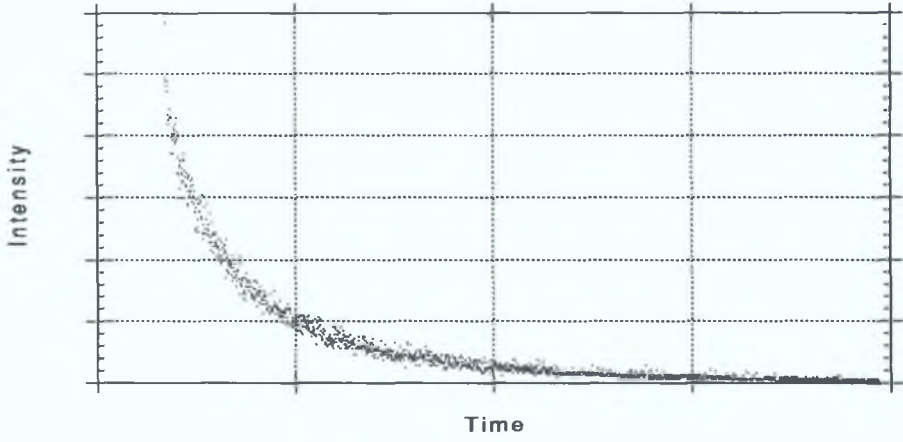


Figure 5.1.3 (b)

Fluorescent Decay with generated "Slow" curve.

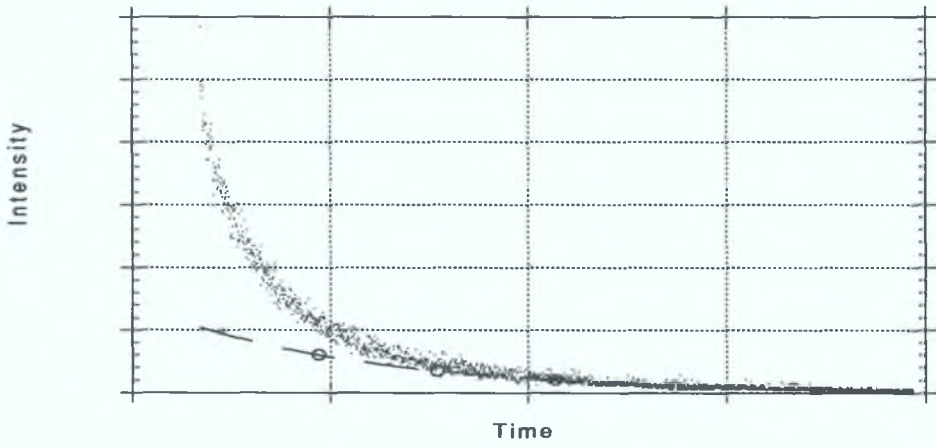


Figure 5.1.3 (c)

Fluorescent Decay and "Stripped" curve.

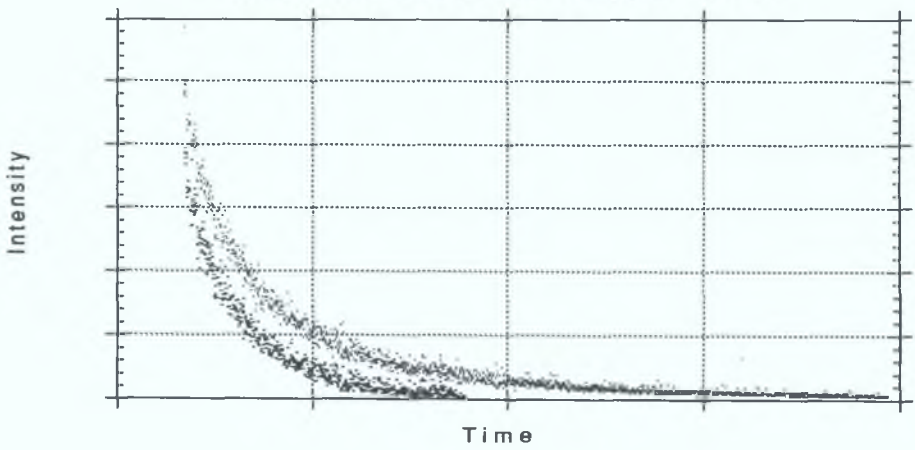


Figure 5.1.3 (d)

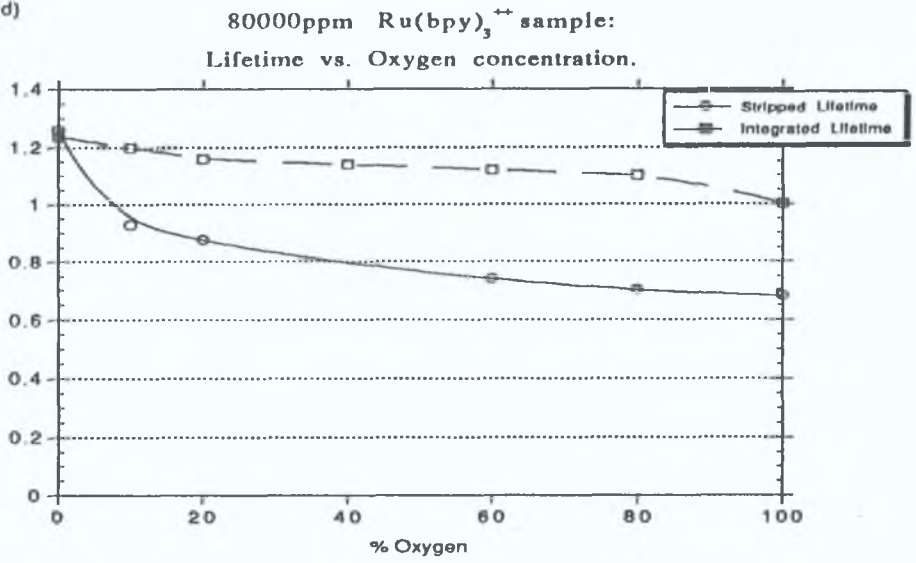
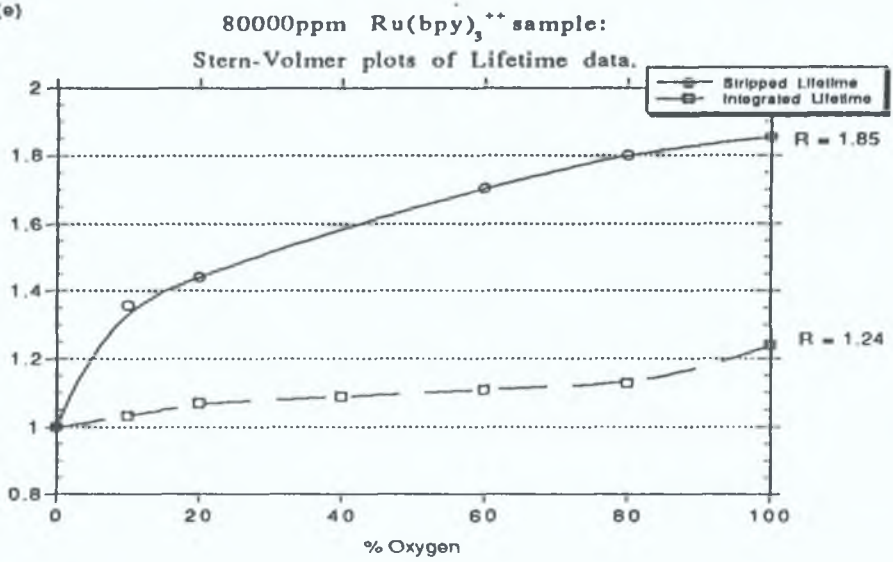


Figure 5.1.3 (e)



data, its equation gives the "fast", quenched lifetime. If this procedure is carried out for data at different oxygen concentrations, fast lifetimes that change with oxygen concentration are obtained, and it is this data that is used in the resulting Stern-Volmer plots.

Figure 5.1.3 (d) shows the variation with oxygen concentration for the lifetime calculated by both the line-stripping and integration methods. Figure 5.1.3 (e) shows the Stern-Volmer plots of this data. From the response to increased quencher concentration, it would seem that the line stripping technique is superior. The integrated lifetime changes very little over the entire oxygen concentration range, and this is reflected in the poor Stern-Volmer plot. This occurs because the method of integration effectively averages the fast and slow components of the decay. It does not take into account the fact that the unchanging, slow portion represents a considerable fraction of the total decay. The integrated lifetime will be dominated by the large unquenched lifetime, and so changes little with increasing oxygen concentration.

The Stern-Volmer plot for the 'line stripped' lifetimes gives a higher R value and thus this method, although more complicated, is a better method of lifetime calculation.

The R value for this plot is 1.85. It is, as expected, lower than that for the fluorescent intensity Stern-Volmer plot. This is because the fluorescent lifetime is not affected by static quenching [1].

From all of the above, it can be seen that the $\text{Ru}(\text{bpy})_3^{++}$ molecule is sensitive to oxygen, but for sensing applications, a greater response would be desired.

5.2 Ru(Ph₂phen)₃⁺⁺

5.2.1 Optimum dye concentration

Figure 5.2.1(a) shows plots of fluorescent intensity versus oxygen concentration for Ru(Ph₂phen)₃⁺⁺ doped samples with dopant concentrations ranging from 10000ppm to 80000ppm. (Note that these concentrations are only half those for the Ru(bpy)₃⁺⁺ samples. This is due to the higher quantum efficiency of Ru(Ph₂phen)₃⁺⁺.) While the ABSOLUTE intensity would appear to increase linearly with increasing dye concentration, the response to oxygen is roughly the same. Figure 5.2.1(b) shows the Stern-Volmer plots of the above, and although the plots are similar, the 20000ppm concentration gives the greatest response, with an R value of 6.7.

This concentration would seem to be optimum, as it is high enough to give a strong fluorescent signal, and certainly low enough to avoid concentration quenching.

Figure 5.2.1 (a)

Ru(Ph₂phen)₃⁺⁺ samples:
Intensity vs Oxygen Concentration.

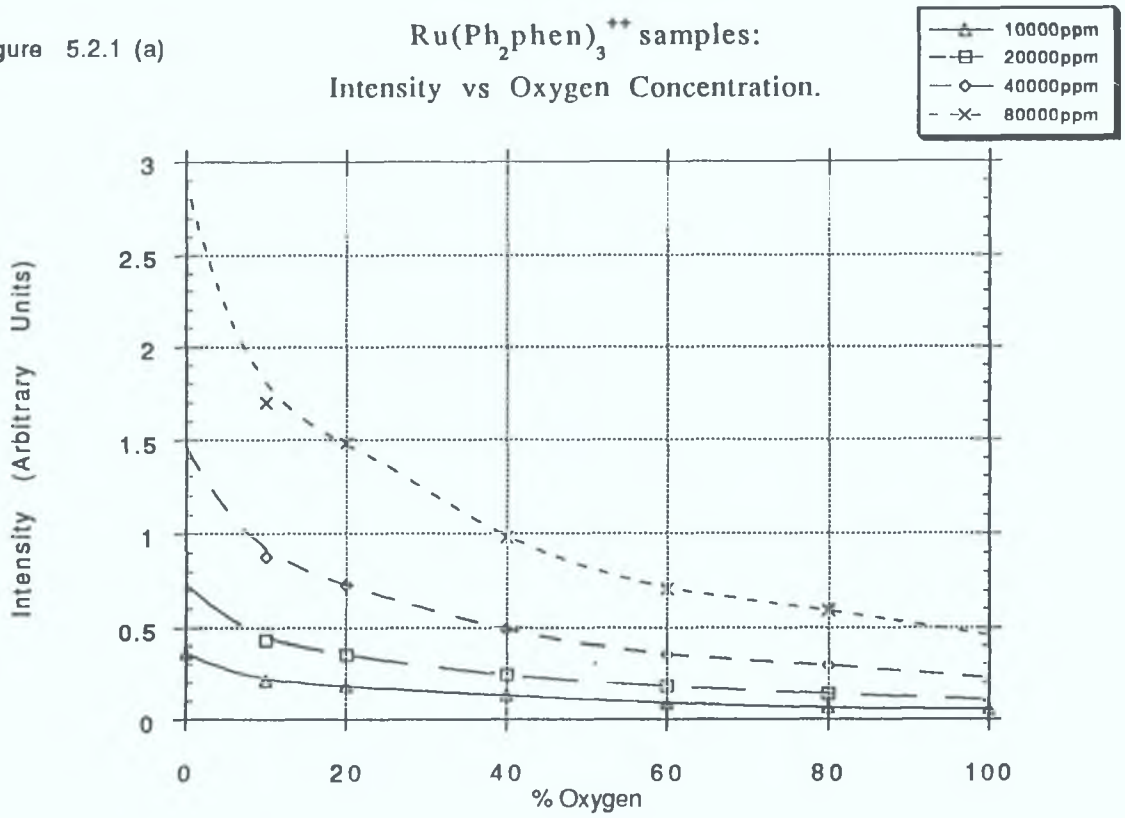
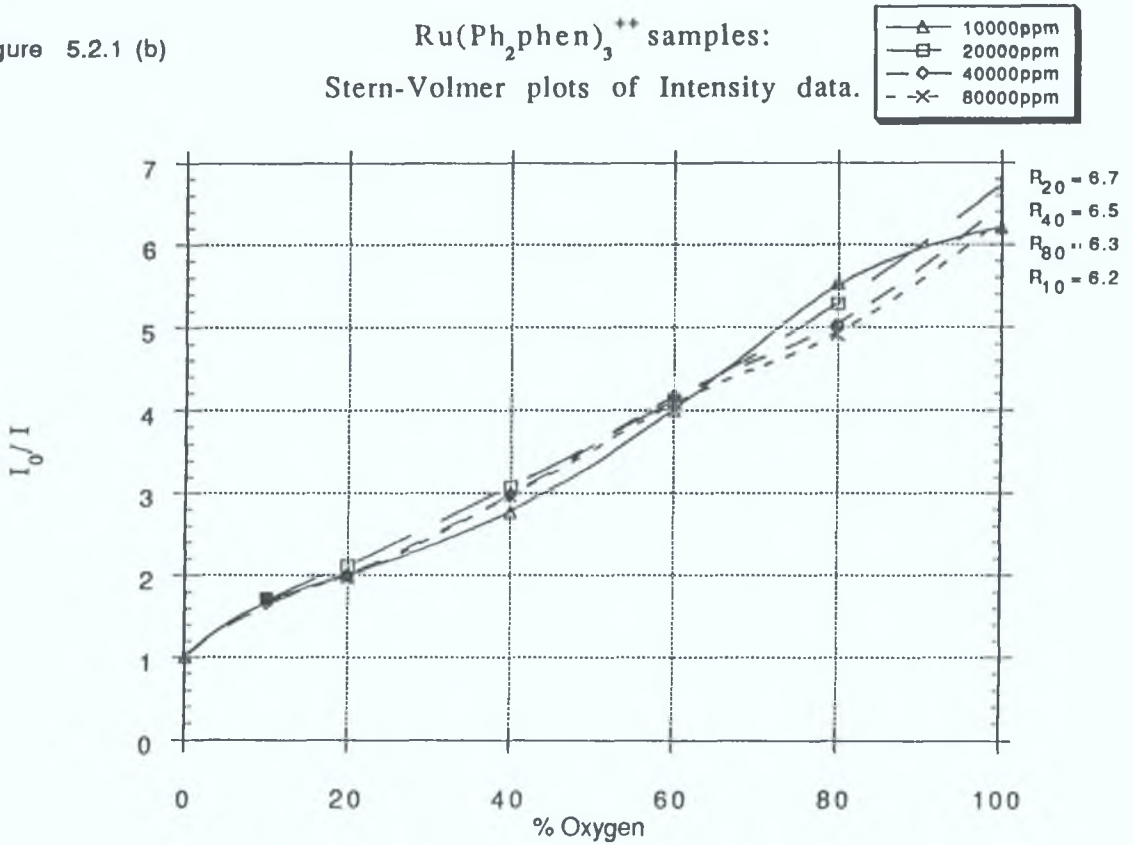


Figure 5.2.1 (b)

Ru(Ph₂phen)₃⁺⁺ samples:
Stern-Volmer plots of Intensity data.



5.2.2 Fluorescent Intensity vs. Oxygen concentration

Figure 5.2.2(a) shows the change in absolute fluorescent intensity for a typical 20000ppm $\text{Ru}(\text{Ph}_2\text{phen})_3^{++}$ sample between 0% and 100% oxygen. There is a much greater drop in intensity than for the $\text{Ru}(\text{bpy})_3^{++}$ samples- under 100% oxygen, the fluorescence drops to just under 15% of its value in the absence of quencher. The change in fluorescent intensity over a range of oxygen concentrations is shown in Figure 5.2.2(b), and the Stern-Volmer plot of this data in Figure 5.2.2(c).

As is obvious from these plots, the response to oxygen is much greater for the $\text{Ru}(\text{Ph}_2\text{phen})_3^{++}$ samples than for those doped with $\text{Ru}(\text{bpy})_3^{++}$, and an R value of 6.7 would indicate that $\text{Ru}(\text{Ph}_2\text{phen})_3^{++}$ is a much more suitable dye for use in an oxygen sensor.



Figure 5.2.2 (c)

20000ppm $\text{Ru}(\text{Ph}_2\text{phen})_3^{++}$ sample:
Stern-Volmer plot of Intensity data.

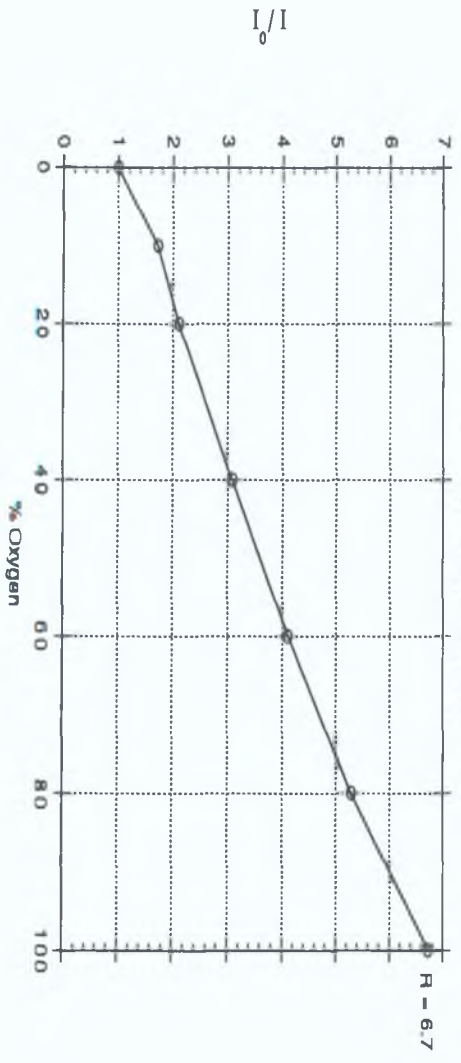


Figure 5.2.2 (a)

20000ppm $\text{Ru}(\text{Ph}_2\text{phen})_3^{++}$ sample:

Change in intensity between 0% and 100% Oxygen.

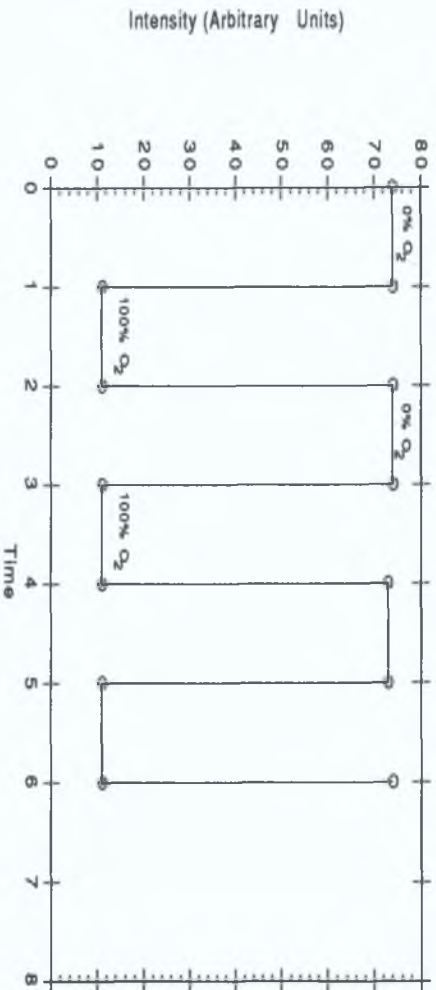
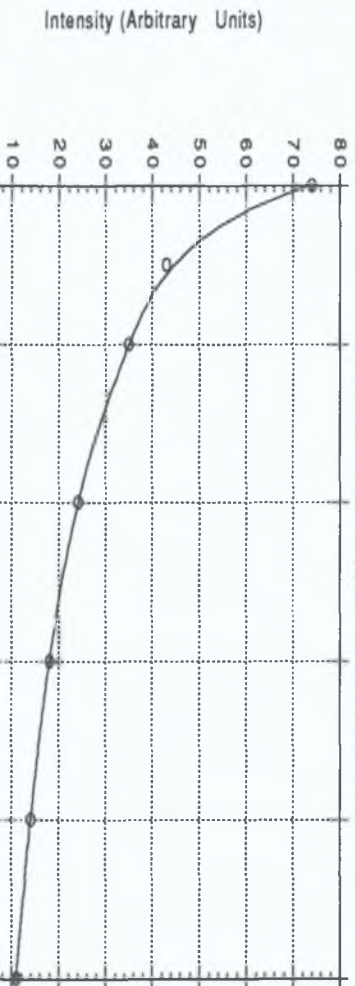


Figure 5.2.2 (b)

20000ppm $\text{Ru}(\text{Ph}_2\text{phen})_3^{++}$ sample:
Intensity vs. Oxygen concentration.



5.2.3 Lifetime vs. Oxygen concentration

Figures 5.2.3(a) and (b) show the lifetime versus oxygen concentration graphs and their corresponding Stern-Volmer plots for a typical 20000ppm $\text{Ru}(\text{Ph}_2\text{phen})_3^{++}$ samples. As before the stripped lifetime gives by far the better plot. As in the case of fluorescent intensity versus oxygen concentration the $\text{Ru}(\text{Ph}_2\text{phen})_3^{++}$ dye is much more responsive to oxygen than $\text{Ru}(\text{bpy})_3^{++}$, with an R value of 5.2.

Again, as expected, the R value for lifetime plots is smaller than for fluorescent intensity.

Figure 5.2.3 (a)

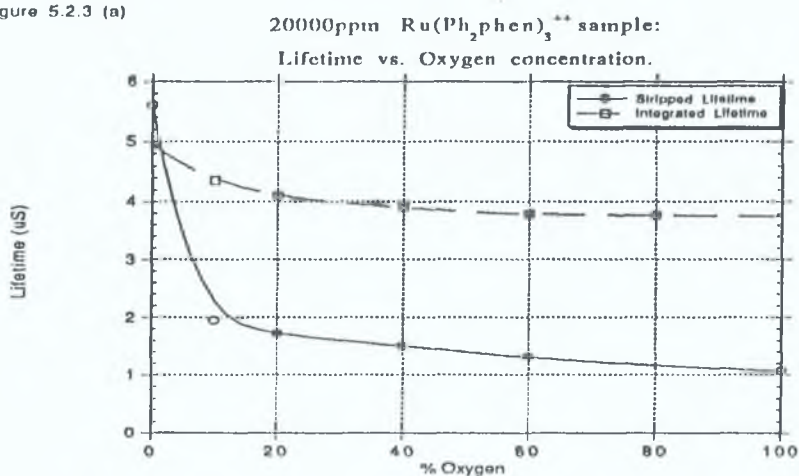
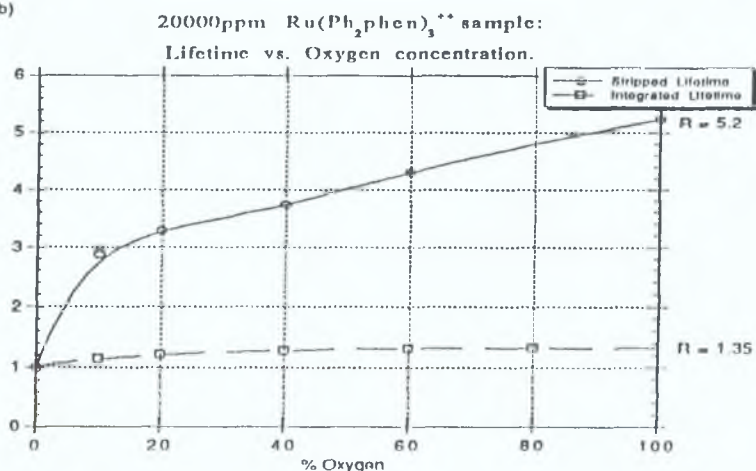


Figure 5.2.3 (b)



5.3 Choice of fluorescent species

Both the change in fluorescent intensity and lifetime for samples doped with $\text{Ru}(\text{Ph}_2\text{phen})_3^{++}$ and $\text{Ru}(\text{bpy})_3^{++}$ are compared here.

Figure 5.3 (a) is a Stern-Volmer plot of intensity data for both fluorescent species. The plot for the $\text{Ru}(\text{Ph}_2\text{phen})_3^{++}$ dye has a much higher R value, indicating a much greater change in fluorescent intensity with increasing oxygen concentration. The same is also true for the Stern-Volmer plot of lifetime data, Figure 5.3 (b).

Figures 5.3 (c), (d), and (e) show how the profile of the decay of a typical 20000ppm $\text{Ru}(\text{Ph}_2\text{phen})_3^{++}$ sample changes with oxygen concentration. (Each is an average of 256 lifetime decays, and is taken directly from a digital storage oscilloscope as described in Chapter 4). There is a very significant change in the profile of the decay as the quencher concentration increases. The 'fast' part of the decay, due to the quenching of the fraction of fluorophores accessible to oxygen, changes markedly. A definite, unchanging portion of the decay is visible, this being the 'slow' decay due to the inaccessible and therefore unquenchable fluorophores.

Figures 5.3 (f), (g), and (h) show the fluorescent decay of an 80000 ppm $\text{Ru}(\text{bpy})_3^{++}$ sample under increasing oxygen concentration. The changes in profile here are much more subtle, indicating a much poorer response to oxygen for $\text{Ru}(\text{bpy})_3^{++}$ samples.

Figure 5.3 (a)

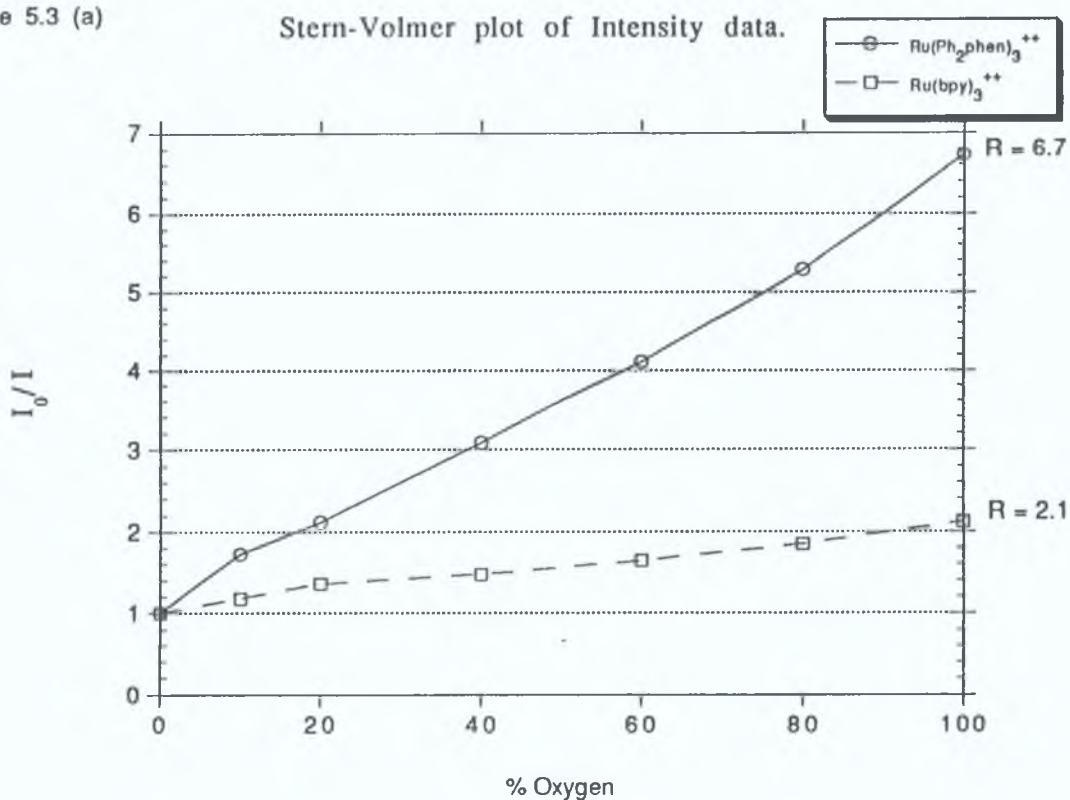


Figure 5.3 (b)

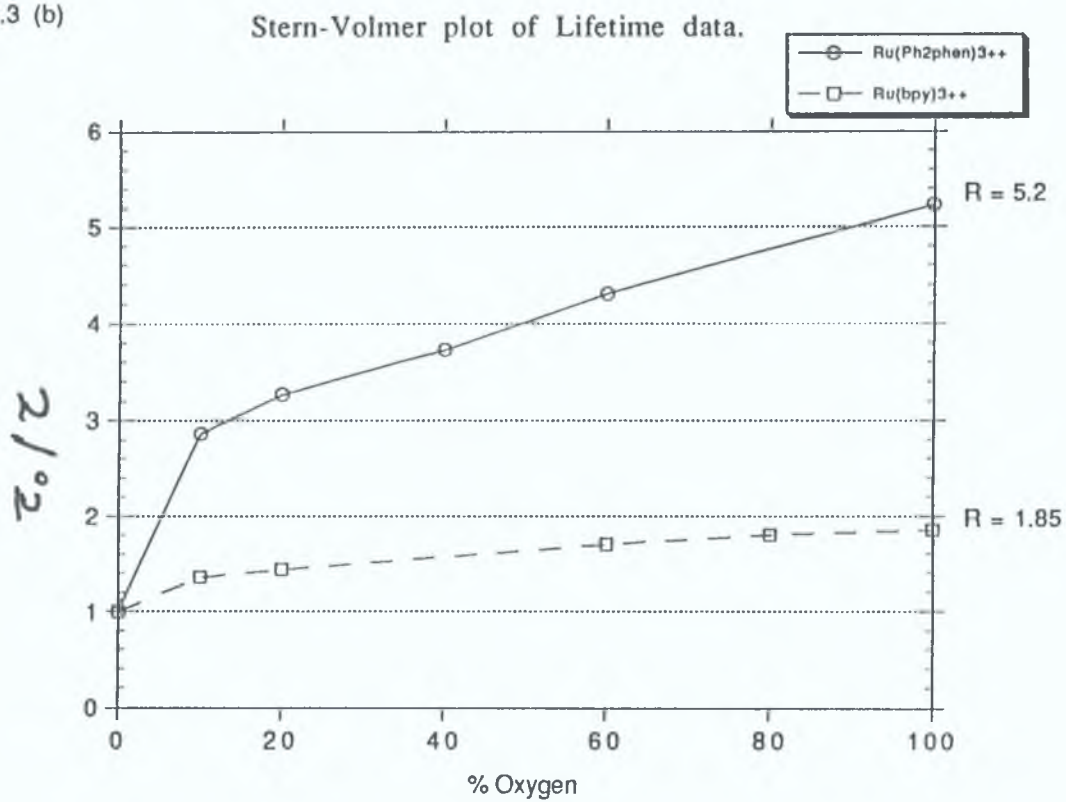


Figure 5.3 (c)

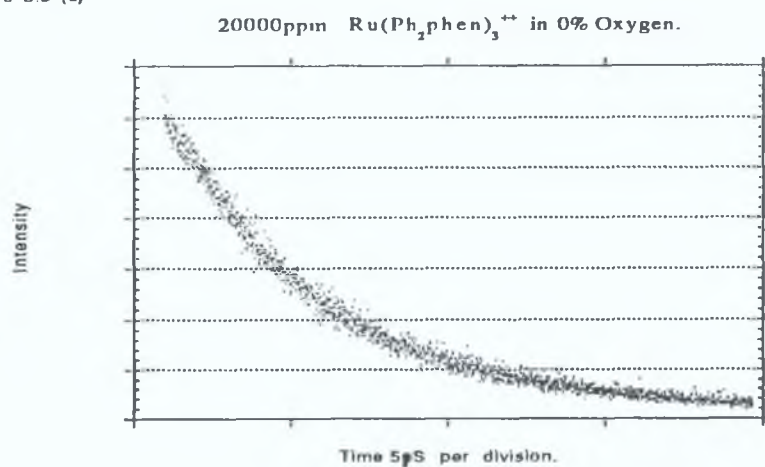


Figure 5.3 (d)

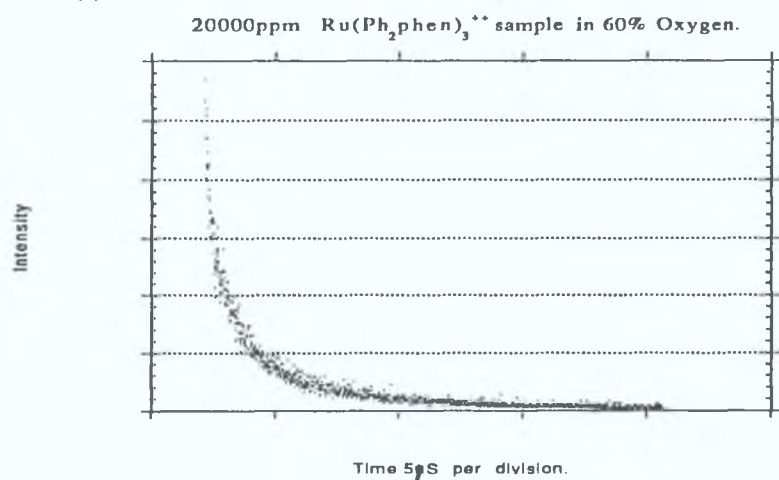


Figure 5.3 (e)

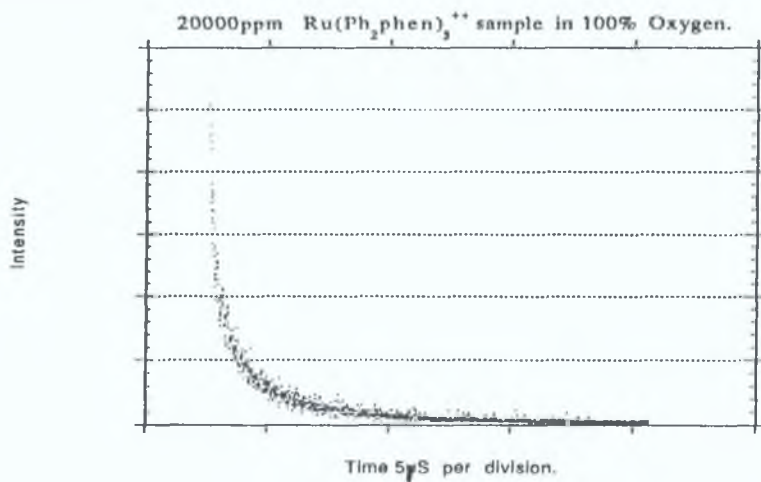


Figure 5.3 (f)

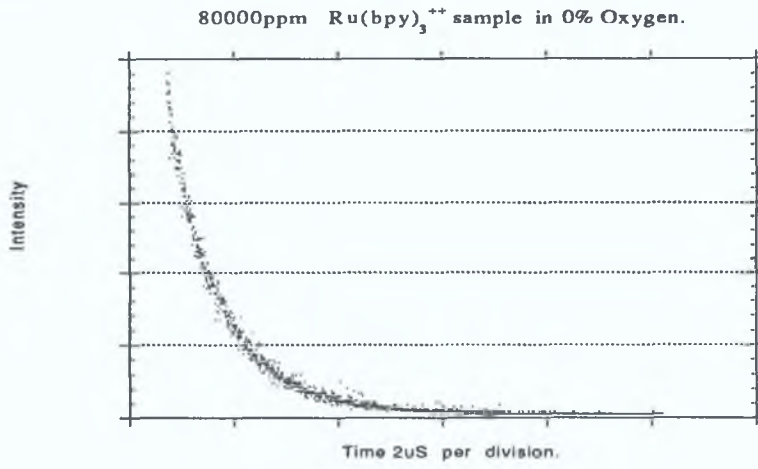


Figure 5.3 (g)

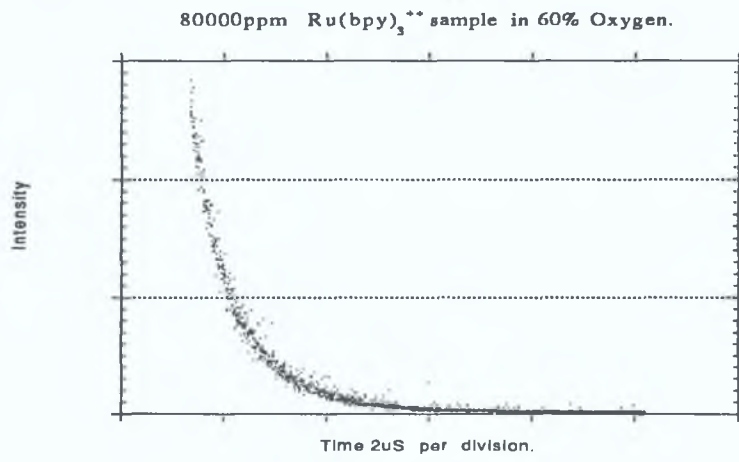
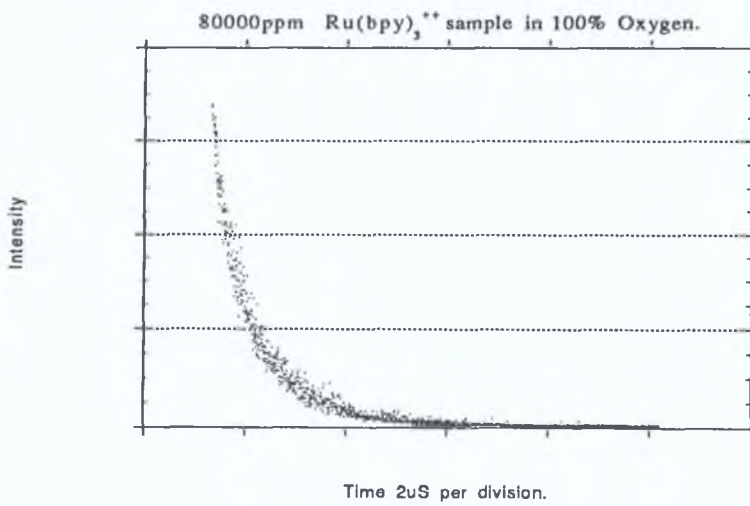


Figure 5.3 (h)



5.4 Aging temperature

Figure 5.4 (a) shows fluorescent lifetime versus oxygen concentration plots for samples aged at two different temperatures, room temperature and 73 °C. Figure 5.4 (b) shows the corresponding Stern-Volmer plots of this data.

As can be seen, the plots are very similar, indicating no significant benefits in aging the sol at the higher temperature, although at this temperature the gels do not have to be aged as long (14 hours at 73 °C as opposed to 24 hours at room temperature).

Figure 5.4 (a)

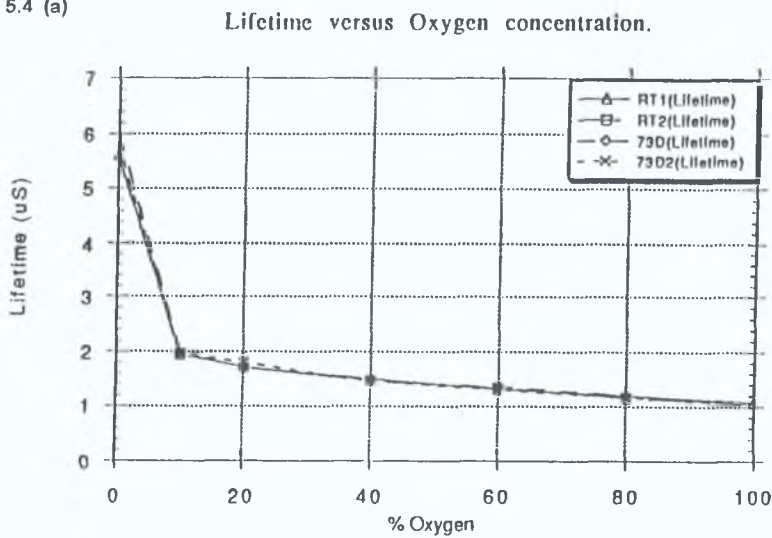
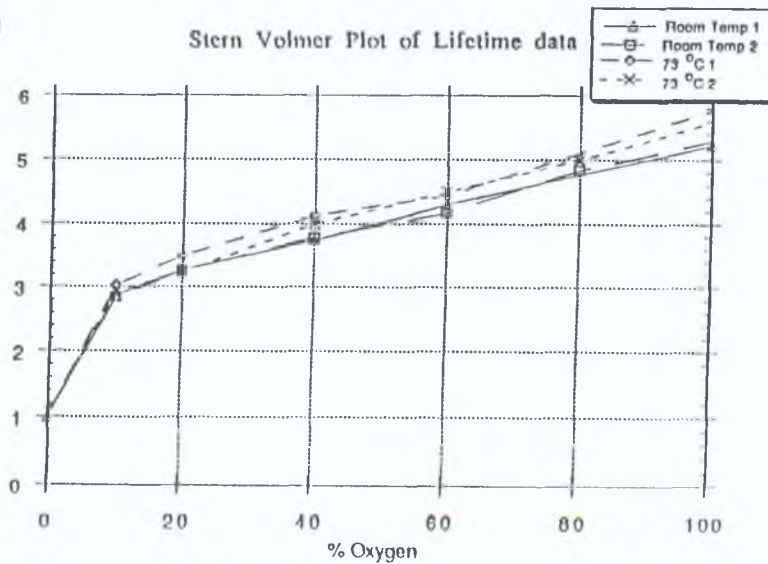


Figure 5.4 (b)



5.5 Lifetime results

Figure 5.5 shows a table of lifetimes for 20000 ppm $\text{Ru}(\text{Ph}_2\text{phen})_3^{++}$ doped samples under varying oxygen concentrations.

'Room Temp.' and '73 Deg' represent averages of data from samples aged at room temperature and 73 °C respectively.

It would appear that the samples prepared at 73 °C give a slightly better response, making them more suitable. However within the error of (+/-) 0.02 uS, the difference is not significant.

The lifetime varies from 5.9 uS in the complete absence of oxygen, to 1.04 uS in 100% oxygen.

Figure 5.5.

% O ₂	Room Temp. Lifetime (uS) (+/-) 0.02 uS	73 Deg. Lifetime (uS) (+/-) 0.02 uS
0	5.6	5.9
10	1.96	1.98
20	1.71	1.76
40	1.48	1.45
60	1.31	1.32
80	1.15	1.16
100	1.06	1.04

5.6 Film performance

In order to see how well the fluorophore was bound within the sol-gel matrix, a leaching experiment was carried out. Using a CW laser, the a 20000 ppm $\text{Ru}(\text{Ph}_2\text{phen})_3^{++}$ doped sample was carefully adjusted so that maximum absolute fluorescent intensity was observed. Next, the sample was removed and allowed to stand under running water for 24 hours. After exposure to water, the sample was dried at 73 °C for 24 hours and again adjusted so that maximum fluorescent intensity was observed. No drop in fluorescent intensity was observed, indicating that there was no significant leaching of the fluorophore from the sol-gel. It should be noted that the positioning and repositioning of the sample before and after exposure to the running water requires a great deal of care to be sure that 'maximum' intensity readings are indeed maximum.

5.7 Summary

From the results obtained in this chapter, 20000 ppm $\text{Ru}(\text{Ph}_2\text{phen})_3^{++}$ doped sol-gel thin films, dipped at 1 mm per second would seem to represent the optimum condition for the sensing of gaseous oxygen. These samples consistently outperformed $\text{Ru}(\text{bpy})_3^{++}$ doped films, and by a very large margin. With regard to the method of lifetime calculation, the line stripping technique proved to be the one of choice, giving a large response to changing oxygen concentrations. The method of numerical integration, although less complex, was found to be unsuitable for the reasons detailed in section 5.3.

The choice of which fluorescent property, intensity or lifetime, to use would depend

on the specific applications of the sensor.

References

[1] "Photophysics and Oxygen Quenching of Transition Metal Complexes on Fumed Silica ," E.R.Carraway, J.N.Demas and B.A.Degraff. *Langmuir*, vol.7, No12, 1991 page 2991.

Chapter 6 Concluding Remarks

6.0 Introduction

This chapter discusses the suitability of the materials and methods developed in this project for use in oxygen sensing applications, and potential future developments

6.1 Fluorescent intensity and lifetime.

As discussed earlier in this project, both the intensity and lifetime of the fluorescent radiation from the samples change in the presence of oxygen.

Figure 6.1 (a) shows Stern-Volmer plots of intensity and lifetime data versus oxygen concentration for a 20000 ppm $\text{Ru}(\text{Ph}_2\text{phen})_3^{2+}$ sample.

As can be seen, the intensity plot shows a greater response over the entire oxygen concentration range. This is due to static quenching (caused by interaction between the fluorophor and the sol-gel substrate to which it is bound), and is not observed in lifetime measurements.

The large number of advantages offered by a lifetime based sensing system (as discussed in Section 2.3) make it more suitable for use as an oxygen sensor.

When measuring the lifetime of the decay, certain things need to be taken into account. It is obvious from figures 5.5.1 (a) through (g) that a two-component (at least) decay is present. The line stripping technique used to calculate lifetime measurements, although complex relative to the method of numerical integration, gave very satisfactory results. It allowed the separation of the two lifetime components, necessary to 'see' the change in lifetime of the fluorophors accessible to oxygen. This is required in a system where only one component of the decay is

Figure 6.1 (a)

Stern-Volmer plot of lifetime and intensity data

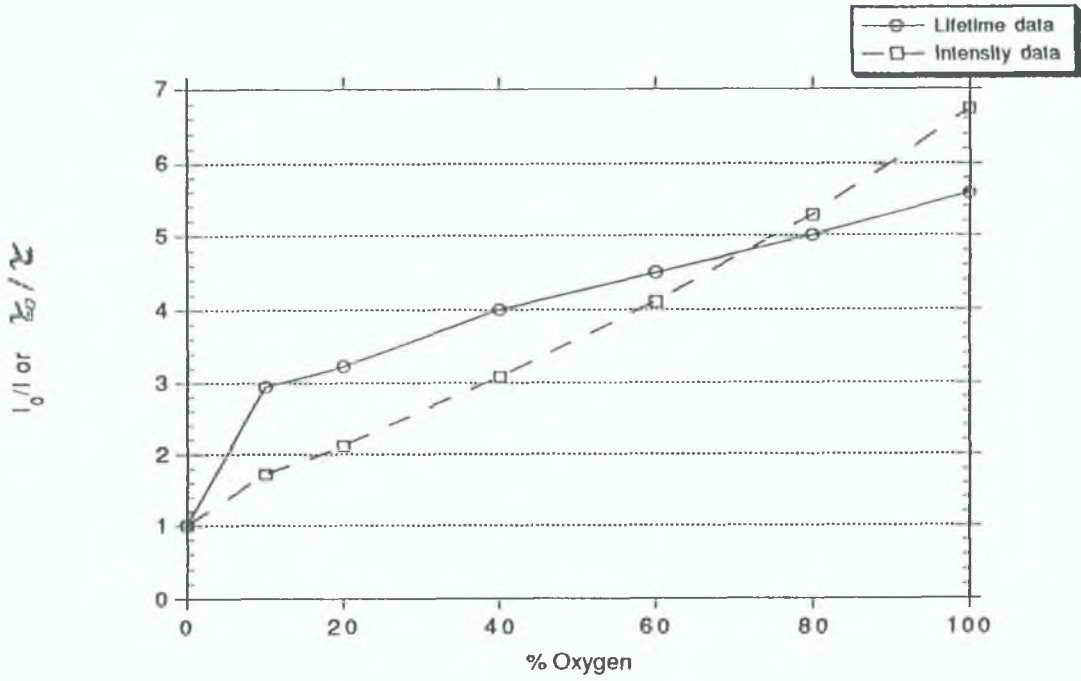
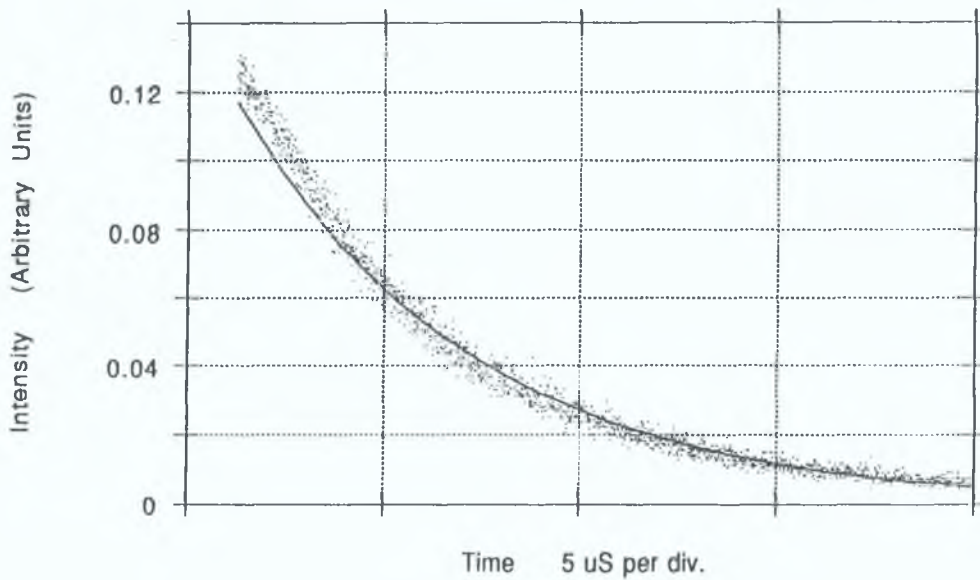


Figure 6.1 (b)

20000ppm $\text{Ru}(\text{Ph}_2\text{phen})_3^{++}$ sol-gel slide in N_2 .



changing.

If the method of numerical integration is used, then as discussed in Section 5.5, the unchanging portion of the decay will dominate and oxygen response will seem poor. The stripping method, however, showed the true response of the system, a response large enough for use in sensing applications.

At least one slight discrepancy exists in this method of calculation, although its effects are not significant. It assumes that the decay is strictly a two component one. This is not completely true, however, as can be seen in Figure 6.2 (b). This shows the decay of a 20000 ppm $\text{Ru}(\text{Ph}_2\text{phen})_3^{++}$ sample under 100% nitrogen (or 0% oxygen). If the decay is only a two component one, then in the absence of quencher, it should behave as a single exponential decay (as the fluorophors both inaccessible and accessible to oxygen should behave the same). However it can be seen that it does not behave exactly like this - the fitted curve does not match exactly.

This is attributed to the fact that the sol-gel support matrix is not completely homogenous. Thus a small percentage of fluorophors will be in a slightly different environment to the others, behaving in a slightly different manner, resulting in the small deviation.

This deviation has no significant effects, and it is concluded that the line stripping method of lifetime calculation is a very suitable one.

6.2 Suitability of the Sol-Gel matrix

From the results obtained in this project, it would appear that a porous sol-gel derived glass is an ideal support matrix for oxygen sensitive fluorescent dyes.

The gels are very simple to produce, requiring relatively inexpensive equipment.

Pre-cursor doping of the gels is merely a simple mixing step, and because the sol-gel process is a low temperature one, very few dopant materials would undergo thermal degradation.

Thin film coatings that were very easy to deposit proved to be very durable, and film properties appeared consistent from sample to sample. The dip-coater constructed played a major part in this, as it allowed samples to be coated at precisely the same speeds.

The porosity of the films was sufficient to allow very fast response times. Response times depend on how quickly the oxygen molecules can diffuse through the pores to reach the fluorophors. In all cases, response times were under 5 seconds (including the time taken to flush the gas cell with new gas concentrations). This means that the sol-gel matrix is ideal for use in real-time, *in situ* measurement applications.

The fact that exposure to running water for 24 hours did not cause leaching of the fluorophor from the matrix shows that the fluorophors are bound very securely within the sol-gel. Hence sensors using sol-gel glass in this way would be suitable for use under harsh conditions.

Finally, the films showed excellent long term stability, with no signs of cracking, flaking or chipping even after five months.

All these factors make porous sol-gel derived glass coatings ideal for use as a

support matrix for sensitive fluorescent dyes.

6.3 Suitability of $\text{Ru}(\text{Ph}_2\text{phen})_3^{++}$

$\text{Ru}(\text{Ph}_2\text{phen})_3^{++}$ proved to be the most suitable of the two compounds investigated.

Its absorption spectrum has a major peak at 460 nm, meaning that it can be excited very easily. There is no need for large, powerful UV excitation sources, in fact a small, cheap blue L.E.D. is sufficient. Its maximum emission peak at 610 nm also means that the fluorescence is easily detected, theoretically with a photodiode.

The large difference in wavelengths (or Stokes shift) between excitation and emission spectra means that complex filtering techniques are not necessary, gel filters are quite sufficient to remove any unwanted scattered excitation radiation.

Like $\text{Ru}(\text{bpy})_3^{++}$, it is selective, being quenched by a small number of chemical species only. Its solubility in ethanol makes it easy to incorporate it into sol-gel glasses. The large change in fluorescent intensity and lifetime of the complex when exposed to oxygen allows for more accurate sensing than $\text{Ru}(\text{bpy})_3^{++}$. (The large change in fluorescent lifetime also means that other lifetime based techniques, such as Phase Fluorimetry, can be used to determine oxygen concentrations.

It is much more highly emissive than $\text{Ru}(\text{bpy})_3^{++}$, and so it is not necessary to use high concentrations of the fluorophor; and the fact that it is less photoreactive makes it a more stable, reliable and long-lived sensing dye.

6.4 Future developments

It would appear that an oxygen sensor based on sol-gel entrapped fluorescent dyes is certainly feasible.

However, the experimental setup used to characterise the compounds and examine their sensing suitability is far too large for any practical sensing applications.

For work in the field, and for commercial viability, a small, cheap, hand-held, portable sensing system would be required. This would require both a small excitation source and detection system.

As stated previously, a blue L.E.D. is sufficient to excite a $\text{Ru}(\text{Ph}_2\text{phen})_3^{++}$ doped thin film, and a photodiode could be used to detect its fluorescence.

If the blue L.E.D. light source is modulated at a certain frequency, then the fluorescence from the sample will also be modulated at this frequency. However, the fluorescence will be out of phase with the excitation source, and this phase shift will change with increasing quencher concentrations. A measure of this phase shift will give a value for the lifetime of the fluorescent decay, and thus the oxygen concentration can be determined. This technique is known as Phase Fluorimetry [1].

The electronics involved in this type of setup are relatively cheap and simple, and small batteries would be sufficient to power such a system.

In this project, the doped thin films were coated on a glass slide, but optical fibres are just as easy to coat.

If the cladding from a section of fibre is removed, and this section coated with a doped film, then the coating can be excited evanescently by focusing light from the excitation source down the fibre. Some of the fluorescent radiation will be reflected back along the fibre, and using dichroic filters, can be separated from the excitation

light. Thus an optical fibre based sensor, offering all the advantages outlined in Section 1.4 is possible. If this can be combined with a phase fluorimetry lifetime measurement system, then a sensor that is truly small, cheap, rugged and portable is certainly obtainable.

The system discussed above is now under development at the School of Physical Sciences, Dublin City University [2] .

References

- [1] "Principles of Fluorescence Spectroscopy "; J.R. Lakowicz, Academic Press, New York, 1983.
- [2] "LED-Based oxygen sensing using evanescent wave excitation of a dye-doped sol-gel coating ". B.D.Mac Craith, G. O' Keeffe, A.K. Mc Evoy, C. Mc Donagh, J.F.Mc Gilp, B.O' Kelly, J.D.O' Mahony and M.Cavanagh. Submitted to Optical Engineering , 1994.